

# Automated System for Optimal Human Awakening



THE UNIVERSITY OF  
**SYDNEY**

Daniel Vogelnest

School of Aerospace, Mechanical and Mechatronic Engineering  
University of Sydney

A thesis submitted for the degree of

*BE(Mechatronics)(Hons)*

November 2012

## **Abstract**

The detection of human sleeping patterns with small, non-invasive devices is an emerging technology. Current implementations achieve improvable results through the use of singular data sources such as acceleration. This thesis focuses on the interpretation of multiple sources of sensory data to achieve greater robustness for optimal wake-up time detection.

To my family and friends

## **Acknowledgements**

I would first like to acknowledge my supervisor Stefan Williams, whose experience and knowledge has been as valuable as the time and effort given to help develop this thesis.

I am grateful for the opportunities that the past year's challenges have presented, both to further my education and for personal growth.

The enthusiastic support and assistance from my family and friends has aided me immeasurably. They've helped me learn to take a step back and smile in times of great stress.

Special thanks go to my mother, Linda Vogelnest, for taking great interest in my work and for her valuable advice from a different perspective.

I greatly appreciate the help from the mechatronics students in my year; and from my biomechatronics lecturer Graham Brooker with his handy advice and inspiring teachings.

# Contents

<b>List of Figures</b>	<b>ix</b>
<b>List of Tables</b>	<b>xi</b>
<b>1 Introduction</b>	<b>1</b>
1.1 Background and Motivation . . . . .	1
1.2 Problem Statement . . . . .	3
1.3 Contributions . . . . .	4
1.4 Outline . . . . .	5
<b>2 Sleep Detection Research</b>	<b>7</b>
2.1 Introduction . . . . .	7
2.2 Sleep and the Circadian Rhythm . . . . .	7
2.2.1 Stages of Sleep . . . . .	8
2.2.2 Influencing Factors . . . . .	9
2.3 Polysomnogram (PSG) . . . . .	9
2.4 Actigraphy . . . . .	10
2.4.1 Sleep/Wake Detection . . . . .	11
2.4.2 Non-Contact Implementations . . . . .	12
2.5 Temperature . . . . .	13
2.6 Heartbeat Correlation with Sleep . . . . .	14
2.7 Heartbeat Detection . . . . .	16
2.8 Electrodermal Activity in Sleep (EDAS) . . . . .	18
2.8.1 Measuring Skin Conductivity . . . . .	19
2.8.2 Electrode Placement . . . . .	20
2.9 Summary . . . . .	21

## CONTENTS

---

<b>3 Design and Implementation</b>	<b>23</b>
3.1 Introduction . . . . .	23
3.2 Sensor Module . . . . .	24
3.2.1 Accelerometer . . . . .	26
3.2.2 Temperature Sensor . . . . .	31
3.2.3 Pulse Oximeter . . . . .	33
3.2.4 Microcontroller . . . . .	35
3.2.5 Wireless Communication . . . . .	39
3.2.6 Power . . . . .	41
3.2.7 Vibration Motor . . . . .	44
3.2.8 Wristband and Electronics Enclosure . . . . .	46
3.3 Computer Module . . . . .	51
3.3.1 Data Collection and Storage . . . . .	52
3.3.2 Processing . . . . .	53
3.3.3 Light and Sound . . . . .	53
3.4 Summary . . . . .	54
<b>4 Processing and Correlation</b>	<b>55</b>
4.1 Introduction . . . . .	55
4.2 Acceleration . . . . .	55
4.3 Temperature . . . . .	57
4.4 Heart Rate . . . . .	58
4.5 Estimate Fusion . . . . .	59
4.6 Summary . . . . .	60
<b>5 Results</b>	<b>61</b>
5.1 Introduction . . . . .	61
5.2 Correlation . . . . .	61
5.2.1 Actigraphy . . . . .	63
5.2.2 Skin Temperature . . . . .	63
5.2.3 Heart Rate . . . . .	65
5.2.4 Fused State Estimate . . . . .	67
5.3 Influencing Sleep . . . . .	71
5.4 Summary . . . . .	72

---

**CONTENTS**

<b>6 Discussion</b>	<b>73</b>
6.1 Sleep State Detection . . . . .	73
6.2 System Design . . . . .	74
<b>7 Conclusions</b>	<b>77</b>
7.1 Contributions . . . . .	77
7.2 Future Research . . . . .	78
7.3 Summary . . . . .	79
<b>References</b>	<b>81</b>

## **CONTENTS**

---

# List of Figures

2.1	Sleep Architecture . . . . .	8
2.2	Machine Learning . . . . .	12
2.3	Temperature vs. Time . . . . .	14
2.4	Temperature and Activity vs. Time . . . . .	15
2.5	Heartbeat Data . . . . .	17
2.6	Reflectance vs. ECG . . . . .	18
2.7	Electrode Placement . . . . .	20
3.1	Modular Design . . . . .	24
3.2	Design Overview . . . . .	25
3.3	Wrist Enclosure . . . . .	26
3.4	ADXL345 Accelerometer . . . . .	27
3.5	TMP102 Temperature Sensor . . . . .	32
3.6	Pulse Oximeter . . . . .	34
3.7	Teensy 2.0 Development Board . . . . .	36
3.8	Microcontroller Operation . . . . .	37
3.9	Microcontroller - Sensor Communication . . . . .	38
3.10	Bluetooth Module . . . . .	42
3.11	Voltage Regulator . . . . .	42
3.12	CR2450 Battery . . . . .	44
3.13	Vibration Motor . . . . .	45
3.14	Vibration Motor Control Circuit . . . . .	45
3.15	Component Layout . . . . .	47
3.16	Enclsosure . . . . .	48
3.17	Component Layout . . . . .	49

## **LIST OF FIGURES**

---

3.18 Mounted Sensors . . . . .	50
3.19 Sensors Protruding from Wristband . . . . .	50
3.20 Enclosure in Wristband . . . . .	51
5.1 Sleep State - Manual Estimation . . . . .	62
5.2 Sleep State Estimation Process - Actigraphy . . . . .	64
5.3 Sleep State Estimation Process - Skin Temperature Correlation . . . . .	66
5.4 Raw Oximeter Data Artefacts . . . . .	67
5.5 Heart Pulses in Oximetry Data . . . . .	68
5.6 Sleep State Estimation Process - Heart Rate Correlation . . . . .	69
5.7 Sleep State Estimate Fusion . . . . .	70
5.8 Light's Influence . . . . .	71

# List of Tables

3.1	Accelerometer Calibration . . . . .	30
3.2	Accelerometer Coefficients . . . . .	31
3.3	Bluetooth Data Rate . . . . .	41
3.4	Power Breakdown . . . . .	43

## **LIST OF TABLES**

---

# **Chapter 1**

## **Introduction**

This thesis is concerned with the detection of human sleep patterns by analysing multiple bodily stimuli. There are many physiological changes that occur in response to alterations in sleep state, however this thesis focuses on the detection of a select few which can be detected through non-invasive means, so as not to unintentionally affect the user's sleep behaviour. The effects of an improved awakening procedure are also investigated. With the gradual introduction of light, vibration and sound the user's sleep patterns may be influenced to induce awakening from an appropriate state of sleep, at an optimal time.

The contributions of this thesis arise from the formulation of a unique approach for the detection of sleep state patterns using non-invasive methods; and the subsequent procedures designed to influence these sleeping patterns and induce an optimal awakening.

### **1.1 Background and Motivation**

Waking up can be a pleasant experience, but usually only when a sufficient amount of sleep has been had - or so most people may think. In actuality, the human sleep cycle is a lot more complicated than this. When we sleep, our bodies transition periodically through a variety of stages, each with their own important physiological functions. If no external influence induces awakening, a person will almost always wake up naturally at the end of one particular stage of sleep - the REM stage. Waking from a deeper sleep state more often results in lasting drowsiness and brief disorientation than when

## **1. INTRODUCTION**

---

awoken at this ‘optimal’ time at the end of the REM stage. The longer one sleeps, the more often this state is experienced; and it is for this reason that the duration of sleep is often considered the deciding factor in how ‘well’ one sleeps (9).

With technological advances, the ability to detect a person’s sleep stage in real-time has become possible. Many physiological processes occur during the different stages in the sleep cycle, each with its own recognisable traits. Sensing just muscle motion can differentiate between some of these stages, and is an emerging commercial technology by itself. Greater accuracy can be achieved with extra sensors to also monitor skin temperature and the heartbeat. As such, it is possible to awaken a person when the previously mentioned optimal sleep stage is detected, even when they have not been sleeping for a long period of time.

There are various methods that can be used to awaken a person, one of the most natural and least jarring being through the presence of light. Light induces a more wakeful state of sleep, and as such it can be used to prime a person for waking (6). This is why it’s much more likely for a person to wake earlier if their bedroom blinds are open, rather than closed to block the morning light. Light by itself can sometimes fully wake a person, but being relatively unobtrusive, it is not a reliable method. For this reason, other methods for waking can be proficiently used in conjunction, such as sound and vibration.

A system integrated with the technology to both detect and affect sleeping patterns and designed to optimally wake the user could revolutionise the current alarm clock market. Unlike a regular alarm clock, such a system would not wake the user during deep sleep, of which the implications are a reduction in induced stress, and an increased productivity after a pleasant awakening.

Being awoken in a more productive state is becoming increasingly important in our time-poor society. The ability to get more done in the morning can improve quality of living by allowing for more personal time. A system that is capable of optimally waking the user presents an opportunity for better health and improvements to the quality of living.

## 1.2 Problem Statement

The objective of this thesis is to develop an automated system to optimally awaken the user. The system utilises a light source to induce a more wakeful state, in conjunction with detecting a person's stage in their sleep cycle; determining the most wakeful state before a user specified wake time. Multiple detection methods are fused for accurate and reliable detection of sleeping patterns.

The primary goals of this thesis are to:

- Detect and predict the user's current stage in the sleep cycle.
- Awaken the user at an optimal time.
- Achieve feasibility as a marketable product.

Detecting the stage of sleep accurately is critical for the system to function correctly. To achieve accurate and robust sleep detection, this thesis investigates a combination of detection methods utilising the sensing of multiple biological parameters; namely:

- Motion - detect muscle motion by monitoring accelerations.
- Heartbeat - monitor changes in blood oxygen content to detect pulses.
- Temperature - observe changes in skin temperature.

The combination of each of these methods produces more accurate and robust results.

The awakening procedure requires two main processes; one to subtly affect the sleep cycle, and one to reliably wake the user. To achieve this the following methods will be used:

- Light - a source of diffuse illumination of dynamically controlled brightness to gradually and subtly increase the wakefulness of the user.
- Vibration - an unobtrusive stimulus of the skin to wake only the user.
- Sound - a relatively invasive backup alarm to ensure the user wakes up.

To achieve feasibility as a marketable product, the system must have the following attributes:

## **1. INTRODUCTION**

---

- Unobtrusive Profile - small size and comfortable to minimise physical awareness of the device.
- Wireless - wires would be hazardous and could interfere with results where movement is restricted.
- Low Power - being wireless, the device must be battery operated, and should be rechargeable, with sufficient capacity to last at least one full night.
- Portable - easily transported, functional in varied environments and with different people.
- Reliable - must reliably wake the user optimally.

### **1.3 Contributions**

The contributions of this thesis arise from the formulation of a unique approach for the detection of sleep state patterns using non-invasive methods; and the subsequent procedures designed to influence these sleeping patterns and induce an optimal awakening.

The major contributions made are:

- Individual sleep state estimates obtained from the analysis of accelerometer, pulse oximeter and temperature sensor data can then be fused to form a single, more robust sleep state estimate.
- An optimal wake-time can be determined from the sleep state estimate fusion process that has been developed.
- The sleep state estimate fusion process can be performed with a small, wireless device attached to the user's wrist that is portable and does not inhibit their natural behaviour.
- Wrist based pulse oximetry and skin temperature measurements can be analysed to determine changes in sleep state.
- The gradual introduction of blue light to a dark environment can be used to reliably increase a person's wakefulness.

## 1.4 Outline

The remainder of this thesis is organised as follows.

Chapter 2 investigates relevant research regarding current sleep detection implementations, and analyses several methods for doing so.

Chapter 3 presents the design and implementation of the automated system developed for this thesis.

Chapter 4 presents the algorithms used to process and interpret the raw data acquired by the system for correlation with sleep events and stages.

Chapter 5 presents the results pertaining to the systems usage.

Chapter 6 discusses the thesis to clarify the meaningfulness of the results and contributions made.

Finally, Chapter 7 presents conclusions and directions for future research in this emerging field.

## **1. INTRODUCTION**

---

# **Chapter 2**

## **Sleep Detection Research**

### **2.1 Introduction**

Before any large project is started, it is of critical importance to review existing literature pertaining to the topics on hand. This facilitates both the planning and implementation stages of the project, and contributes to its efficiency and effectiveness.

This chapter discusses the literature reviewed during the development of this thesis, with focus on human physiological behaviours during sleep, relating especially to motion, skin temperature and heart rate. Several detection methods are introduced, and existing research and development discussed.

### **2.2 Sleep and the Circadian Rhythm**

Sleep is a state of reduced consciousness, where almost all voluntary muscles are inactive, and sensory abilities are damped. Sleep aids the development of the brain, growth and healing; as well as memory processing (32). No animals have been found that do not require sleep without experiencing serious repercussions, yet the reason for its essentiality is still a topic of intense research (9).

Sleep naturally occurs periodically, and is heavily influenced by the biological clock. A biological circadian rhythm is defined as a process that oscillates once a day, even without environmental cues such as light and temperature (endogenous), but can still be adjusted by such cues to allow for variations in time with location (entrainable) (29). The human biological clock is a circadian rhythm that is of significant importance in the regulation and coordination of metabolic processes. The periodic release of hormones

## **2. SLEEP DETECTION RESEARCH**

---

synchronises the peripheral clocks of various organs, whereby the timing of changes in wakefulness, body temperature, thirst and appetite are controlled (29).

The biological clock also plays an integral role when a person is asleep. There are various stages of sleep that are associated with different physiological, neurological, and psychological functions, which are required to occur periodically for varying durations. The biological clock regulates the timing of these functions to such a degree that the stages of sleep in the sleep cycle occur in a predictable pattern (as seen in figure 2.1).

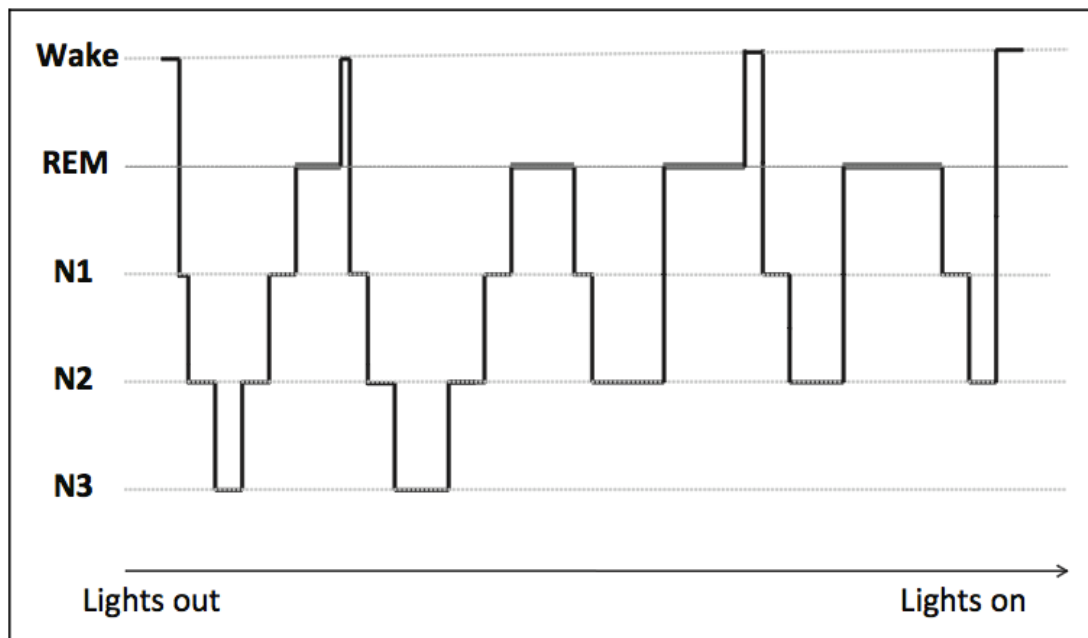


**Figure 2.1: Sleep Architecture** - Normal adult hypnogram demonstrating usual sleep stage transitions (15).

### **2.2.1 Stages of Sleep**

The stages in the sleep cycle are categorised as REM (Rapid Eye Movement) and Non-REM. The Non-REM stage consists of three progressively deeper sleep stages termed N1, N2 and N3 (N3 being the deepest), where the cycle normally repeats in the order N1 to N2 to N3 to N2 to REM (30). Deep sleep (N3) occurs for longer periods of time earlier in the sleep cycle, while the REM stage is more common later in the cycle before naturally waking.

## **2.3 Polysomnogram (PSG)**

---

The Non-REM stages of sleep are classified by the frequency of the brain's waves, but each stage has other distinguishable features. N1 is associated with some loss in muscle tone, as well as sudden twitches (4). Muscular activity, heart rate, and body temperature decrease in N2, and further again in N3. During a typical night of sleep, about four cycles of sleep occur.

The effects of interrupting the normal sleep routine can be significant. There are various forms of sleep deprivation, the most common being chronic partial sleep deprivation, and erratic sleep schedules. Sleep deprivation negatively effects cognitive and emotional processes, and is associated with an increased likelihood of accidents, aggression, depression, diabetes, obesity, and cardiovascular health problems (11).

### **2.2.2 Influencing Factors**

The biological clock is prone to both long and short term disturbances to sleeping patterns. The sources of these disturbances can include noise, temperature, motion, and light; anything that can interrupt the sleep cycle.

Light plays a very important role in the sleep cycle. The presence of light at the end of the sleep cycle can advance the biological clock; the degree of which is dependant on the intensity, exposure time and colour of the light. Melanopsin is a photopigment found in the eye's retina which helps regulate the biological clock, and is most responsive to blue wavelengths (peak at 484nm) of light (21). The signals from melanopsin are received by the suprachiasmatic nucleus (SCN) in the brain, which in turn inhibits the production of the hormone melatonin that causes drowsiness and lowers body temperature.

## **2.3 Polysomnogram (PSG)**

The detection and monitoring of the sleep cycle is generally used to diagnose many types of sleep disorders, typically through the use of a polysomnogram. Polysomnography is generally performed in a sleep laboratory where the sleep cycle is detected through the combination of various techniques such as:

- Electroencephalography (EEG) monitors brain activity, showing the brain wave frequencies that are used to classify the various stages of sleep.

## **2. SLEEP DETECTION RESEARCH**

---

- Electrooculography (EOG) detects the eye movement that is characteristic in the REM stage of sleep, and the lack of in Non-REM stages.
- Electromyography (EMG) measures muscle tension and movement.
- Electrocardiograph (ECG) detects electrical activity of the heart, from which heart rate and potential abnormalities are gathered.

All of these techniques measure bio-electrical signals, requiring electrodes to be wired and attached to the body, inhibiting natural movements. Other sensors are sometimes used in conjunction such as cameras, microphones and pulse oximeters. While computers are often used for some of the processing, sleep technicians generally do the ‘scoring’ of the stages of sleep.

### **2.4 Actigraphy**

During the sleep cycle, the body’s motion varies with the stage of sleep. An actigraph device senses this motion, the degree and type of which can be categorised into corresponding relationships with specific stages of sleep. While it does not provide the level of detail obtainable from a polysomnogram, the advantages of actigraphy over polysomnography include:

- Non invasive - can continuously record data for extended periods with minimal interference with the user’s motion and routine’s.
- Non-fixed environment - doesn’t require the user to go to a sleep laboratory, and is suitable for use in the user’s own home where their sleeping behaviour is less likely to be altered.
- Cost effective for diagnosing some sleep disorders such as insomnia, circadian disturbances, and periodic limb disorder (7).

Despite the simplicity of actigraphy, it is able to detect the sleep cycle with approximately 80% to 90% of the cases, depending on the method and algorithms used (24).

To measure motion, actigraph devices utilise accelerometers. The device is generally placed on the wrist (2), but some implementations are used on the ankle or trunk.

## **2.4 Actigraphy**

---

Various studies on the effectiveness of each location show differing results, some found no difference, while others suggest the dominant wrist performs best, closely followed by the non-dominant wrist, then the ankles and trunk with lowering degrees of effectiveness respectively. Voluntary human movement rarely exceeds 3-4 Hz, and the involuntary movements like tremors and shivering rarely exceed 5Hz, except in younger people whose movements can reach 11Hz (2).

Actigraphy can be affected by various artefacts, such as breathing motions (can be corrected by appropriate data filtering); postural effects (e.g. lying on an arm; typically negligible influence); and external motion (e.g. sleeping in a moving vehicle; should be avoided)(2).

### **2.4.1 Sleep/Wake Detection**

Some implementations of actigraphy only require the differentiation between sleep and wakefulness. A method to achieve this is to model the accelerometer data as a combination of two data distributions; a shifted Maxwell distribution resembles purposeful motion data from a wakeful state, and a Poisson distribution fits the short duration motions common in sleep. The disadvantage of this method is that it can only be processed after a set of data is collected, but results have a high correlation with sleep diary entries (24). More commonly, simple activity counts are determined through digital integration of raw accelerometer data over 30 or 60 second epochs. These activity counts are used to differentiate the wake and sleep states, still with greater than 85% agreement with PSG results (22).

One example of a research device utilising this method is the Actiwatch-L, which additionally incorporates a photodiode to monitor light intensity. Its accelerometer has a sensitivity of 0.05g and is sampled at 32Hz, filtered through with a bandwidth of 3 to 11Hz - unlike other commercially available devices which commonly have a smaller and lower bandwidth of 0.25 to 3Hz. The Actiwatch-L's unusual bandwidth was designed to remove some artefacts of gravity in the sensor data (34). Filtering the accelerometer signals is necessary to help remove unwanted data and noise.

A unique method for the prediction of the sleep cycle is through the use of an actigraphy unit that communicates with a remote database, comparing actigraphy data and user physiological parameters with data from similar users. The database is updated

## 2. SLEEP DETECTION RESEARCH

---

with machine-learning algorithms producing greater prediction accuracy. This process is depicted in figure 2.2.

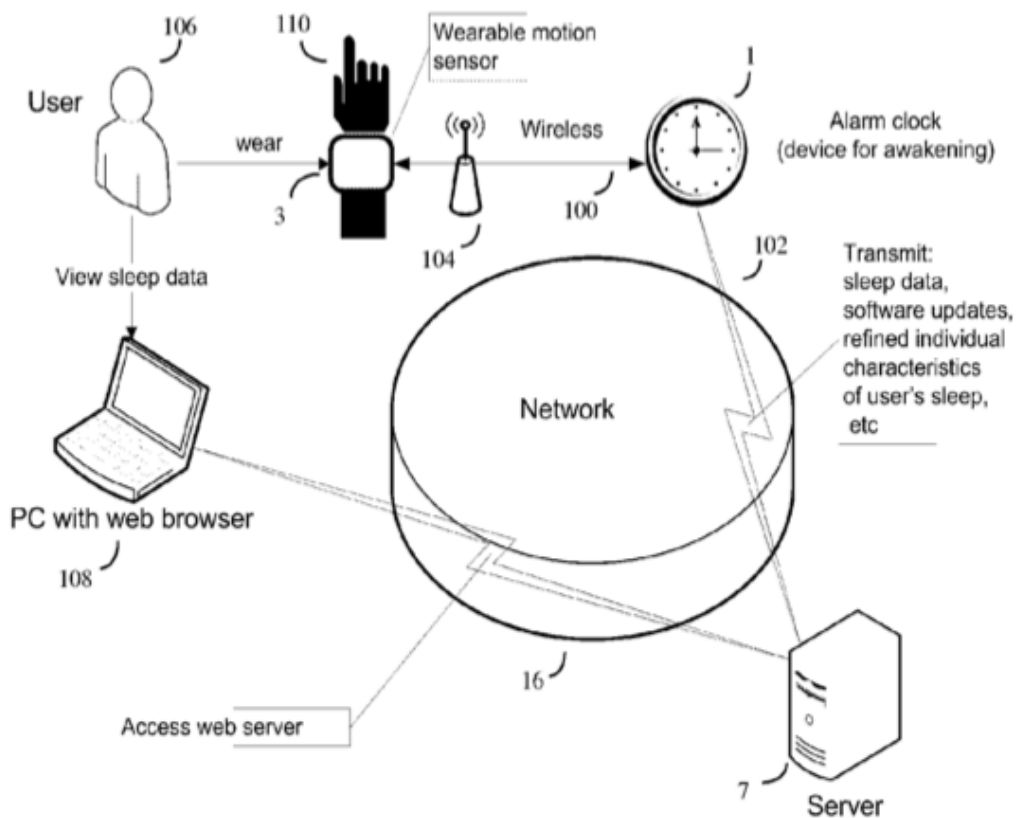


**Figure 2.2: Machine Learning - Database machine learning based method and system for sleep monitoring, regulation and planning (33).**

### 2.4.2 Non-Contact Implementations

In general, actigraphy is performed with motion detectors physically attached to the user's body; but motion data can also be gathered from mattress movements. In a trial performed by Andrew McDowell (19), six 3-axis accelerometers were attached to a mattress from which sleep/wake stages were determined. Digital integration and time above threshold methods were used to obtain activity counts as with some of the contact methods, but with the addition of a random forest classifier (a type of machine learning algorithm) using features calculated from the static accelerometers. It was found to

produce a sleep/wake classification accuracy of 92% (19). The commercial iPhone application “Sleep Cycle” functions using a similar process, utilising the iPhone’s inbuilt accelerometers.

Another non-contact actigraphy implementation utilises load cells installed under the corners of a bed. Movements are detected through interpretation of the forces sensed, and wakeful motions can be detected with an average error rate of 3.22% (1).

The advantages of these non-contact methods is the slight reduction in obtrusiveness to the user’s sleep (down from wearing a wrist band), and the simplification of motion detection. On the other hand, they are more complicated to install and do not acquire as much information as most other methods.

## 2.5 Temperature

Body temperature is strongly linked to the human metabolism and circadian rhythms in sleep. Heat production follows a circadian rhythm, as does heat loss from the body. During sleep, the body decreases heat production, and increases heat loss through increased blood flow in the skin - often to a level rarely seen during wakefulness (35). Figure 2.3 shows the average human temperature curves measured under constant conditions. The distal skin temperature (as measured on the wrist) is most indicative of heat loss through the skin, and contrasts with proximal skin temperature (as measured on the torso).

In contrast, figure 2.4 portrays synchronised distal and proximal skin temperatures during sleep, as measured over three days. However, both sources of data show that distal skin temperature increases when transitioning from wakefulness to sleep, and decreases when the transition is reversed; the skin temperature drops when becoming increasingly wakeful.

Note the activity measures in this experiment are performed with actigraphic techniques, and reflect the behaviour discussed in section 2.4. The fact that skin temperature on the wrist increases during sleep with the increase in skin blood flow is also advantageous for measuring the pulse with oximetry techniques. The extra blood means greater volume change with heart beats. Consequently, greater changes in reflected/absorbed light occur, and the detected light signal is more likely to be significant compared to signal noise, allowing for more robust pulse detection.

## 2. SLEEP DETECTION RESEARCH

---

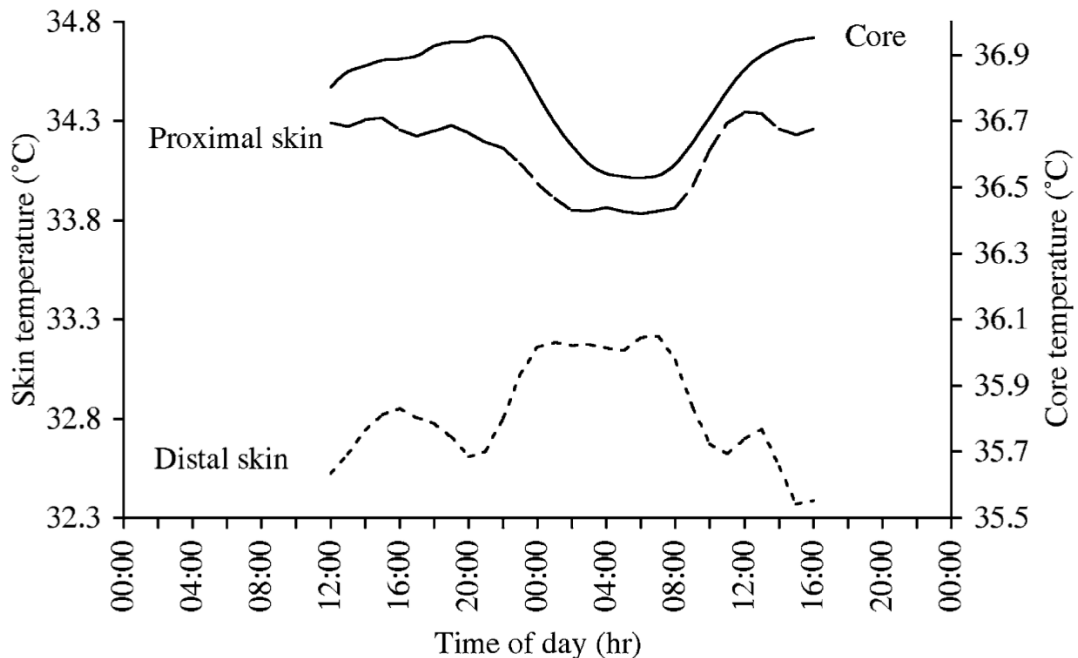


**Figure 2.3: Temperature vs. Time - Increased heat loss during sleep (35).**

Skin temperature typically ranges from 27°C to 36°C (8), dependant on various factors; primarily environmental conditions, activity levels, wakefulness, body mass, fitness and heart rate.

Conversely, it has been observed that the state of sleep can be manipulated through the control of skin temperature. Warming distal skin results in increased wakefulness, but can also be controlled to increase intervals of individual sleep stages (e.g. the REM stage) as desired (13).

## 2.6 Heartbeat Correlation with Sleep

The heartbeat has several features that can be correlated to different stages in the sleep cycle. For example, during deeper sleep the heart rate drops, while in the REM stage, the heart rate tends to vary more significantly (and more frequently) than in any other stage.

The average and standard deviation of the interval between heartbeats can be used to determine the state of sleep (20). These values however can vary during different

## 2.6 Heartbeat Correlation with Sleep

---

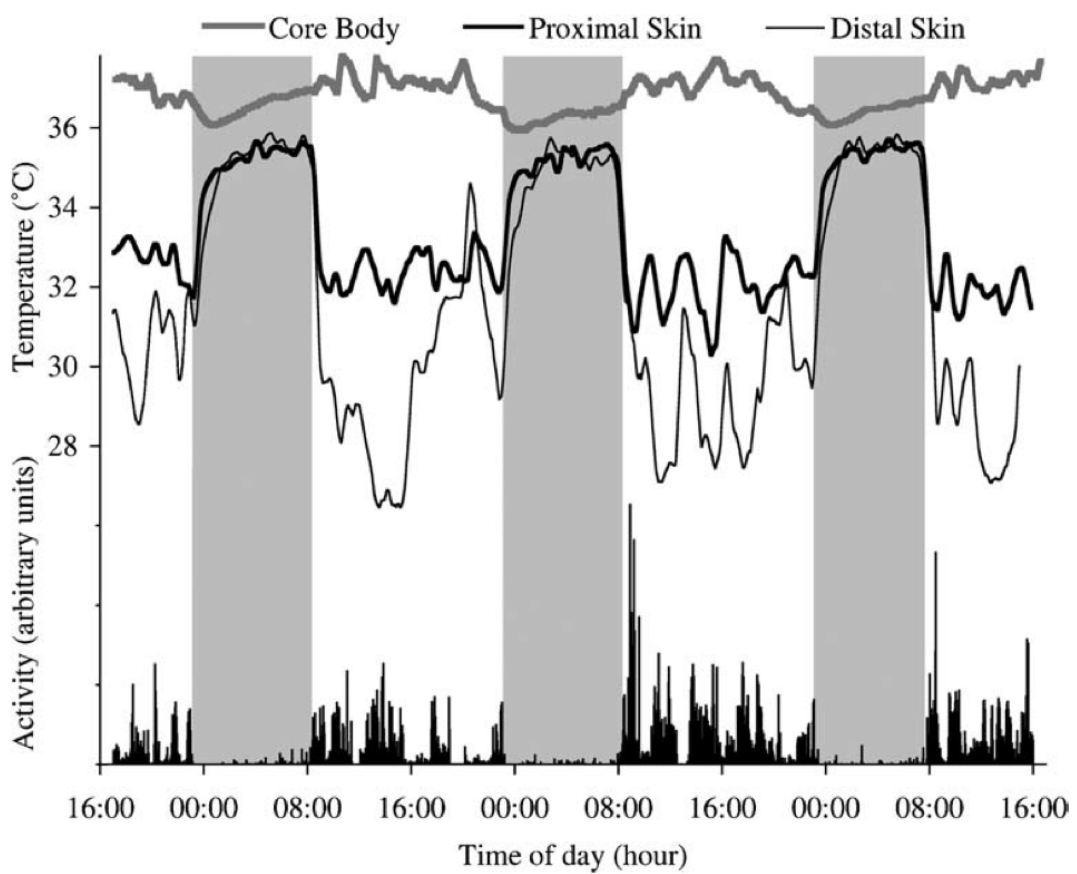


**Figure 2.4: Temperature and Activity vs. Time -** Grey columns represent sleep (35).

## **2. SLEEP DETECTION RESEARCH**

---

occurrences of the same stage of sleep, and as such a more complex detection algorithm is often necessary to correlate heartbeat with sleep in greater detail than simply the wake-sleep cycle (23).

A recently developed method that accounts for these changes utilises the de-trended fluctuation analysis (DFA) method (3). DFA has successfully been applied in diverse fields such as DNA sequences, heart rate dynamics, neuron spiking, human gait, long-time weather records, cloud structure, geology, ethnology, economics time series, and solid state physics (16).

Other techniques for the detection of correlations like the autocorrelation function and the power spectrum are not suited for a non-stationary time series (changes slowly or intermittently from background influences) such as that of the heartbeat interval during sleep (16).

The DFA procedure consists of four steps (16):

1. Determine the cumulative sum profile with acquired data.
2. Segment the profile into equal lengths. For profiles of odd lengths, this process is performed twice, grouping data starting from both the first and last element.
3. Determine the variance of the least squares fit for each data segment.
4. Square root the average of all segments to acquire the fluctuation function,  $F(n)$ .

Figure 2.5 shows some heartbeat data processed with this method, which can be used to differentiate between the stages of sleep. While using DFA for heartbeat analysis is relatively intensive, it often produces good results pertaining to the accuracy and stability of the heart rate.

### **2.7 Heartbeat Detection**

The heartbeat is most commonly detected using an electrocardiogram (ECG) for sleep cycle monitoring. An ECG measures the electrical activity of the heart through properly placed electrodes, producing in-depth information regarding the different components of a heartbeat and the operation of the heart as a whole.

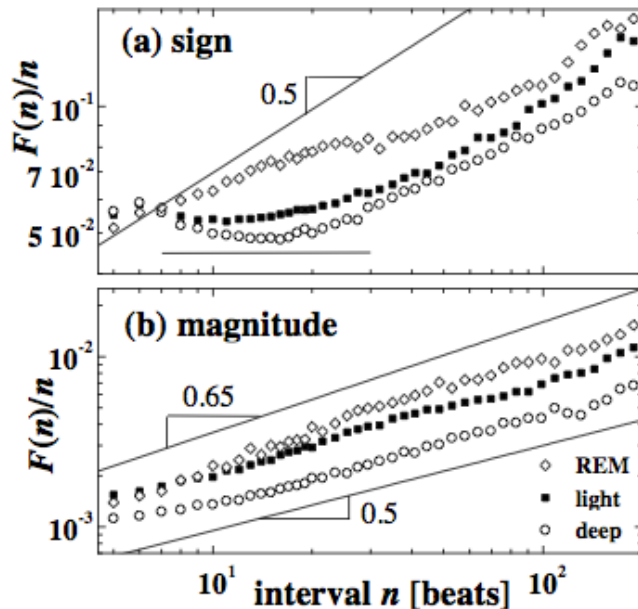


**Figure 2.5: Heartbeat Data** - Fluctuation functions for different sleep stages (16).

The requirement of multiple electrodes can intrude on the subject's freedom of movement and comfortability, and as such is unsuitable to be confined into a small device that could be situated only on the wrist.

In comparison, pulse oximetry can be performed with a small, self contained device. Pulse oximetry is a method for measuring the blood oxygen content, which has a component that oscillates with the heartbeat. The principle behind the detection of the blood oxygen content is that a volume of optically absorbent/transmitting substance (such as SPO<sub>2</sub> in blood) will absorb and reflect to a degree related to its volume. Hence, by transmitting a light to the blood, and detecting what is not absorbed gives a measure of the oxygen content within.

There are two types of pulse oximetry: absorption and reflectance. Both utilise a light source and a light detector, but the placement of the two differs. With absorption, the detector is located opposite the light source, with a thin part of the body between which enables the measurement of light that is not absorbed by the blood and tissue. Reflectance, however, has the detector located next to the light source, and measures the amount of light that is reflected from the blood and tissue. The advantage of the reflectance method is that it does not require a thin body part such as a finger or

## 2. SLEEP DETECTION RESEARCH

---

earlobe, and can be used on locations such as the feet, forehead or wrist.

This optical method can achieve average sensitivities and precisions of 98.03% and 97.62% respectively (31). Figure 2.6 demonstrates this relationship between ECG and optical methods.

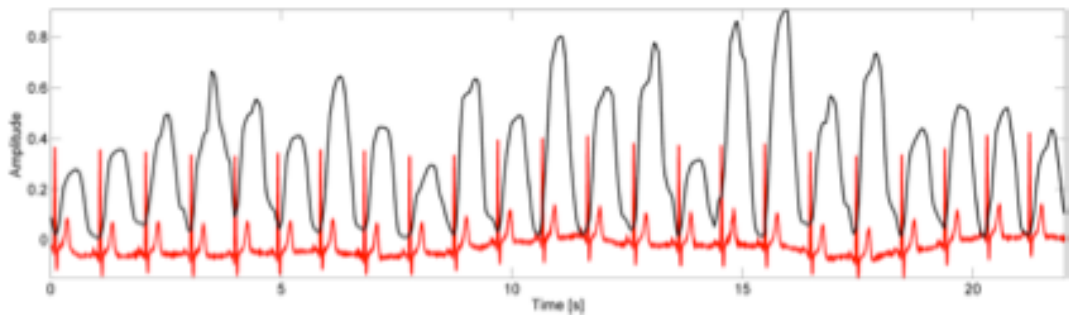


**Figure 2.6: Reflectance vs. ECG** - Comparison of ECG (red) with optical reflectance (31).

## 2.8 Electrodermal Activity in Sleep (EDAS)

One of the body's physiological responses to mental, emotional or physical arousal is an increase in sweat secretion. Sweat, being a weak electrolyte, is a good conductor, and as such its presence results in the formation of many low electrically resistant parallel pathways - increasing skin conductivity (18). This is of particular interest as the degree and spontaneity of electrodermal activity (EDA) during sleep is definitively correlated to the stages of sleep.

EDA is most abundant during the deep sleep N3 stage, consistently decreasing during the six minutes preceding a REM stage which entails minimal EDA (5). The few occurrences of EDA during REM have been shown to correlate with bursts of eye movement, and high dream emotionality. On a higher level, EDA occurs significantly less frequently during the first full sleep cycle and after the third (17).

While ambient temperature and humidity do have an effect on EDA, the variance in characteristics is relatively low compared to the differences resulting from variation in subject age and sex (36). Women generally have greater sweat gland density, with delayed and less profuse sweating than males. This corresponds to females having a higher tonic (baseline conductivity) EDA and reduced reactivity to stimulation than

## **2.8 Electrodermal Activity in Sleep (EDAS)**

---

males (14) (27). However, the EDA differences between sexes are not easily distinguishable in older people. Older people also have lower resting skin conductance levels, but EDA responses and patterns remained the same as for younger subjects (10).

Regardless of the demographic, skin conductance behaves predictably and has a strong relationship with the sleep cycle, and can be used to determine current stages of sleep, and predict imminent changes.

### **2.8.1 Measuring Skin Conductivity**

There are two main methods for detecting EDA: actively measuring skin conductance, and passively measuring skin potential. The latter is regarded as more a reflectance of physiological changes because of its passivity - a current is not applied as for skin conductance. It is also well suited for extended use as electrode polarisation is minimal, it is not affected by variations in electrode contact area, and can be measured by using simpler AC bioamplifiers (27). However, measuring skin conductivity is often preferred due to the biphasic nature of skin potential responses, making amplitude measurements difficult to interpret. Skin potential is also more prone to vary with changes in skin hydration (12).

Skin conductance is measured by applying a constant voltage between the two electrodes. Any change in skin conductance results in a change in current flow between the two electrodes. In comparison to skin resistance methods, this technique uses both electrodes placed on active sites; which is called bipolar measuring. An appropriate value for the constant voltage applied has been found to be 0.5V, and is almost unanimously used in all skin conductance measurement implementations (28).

Electrodermal activity is comprised of two main components: tonic and phasic (26). The tonic component is the skin conductivity baseline; a low frequency value that can oscillate with a period of days. The phasic component is of a much higher frequency; rapidly fluctuating in relation with the persons level of arousal. It is the phasic component that is of most use for correlation with the sleep cycle, and the behaviour of this component does not vary greatly between people. However, the tonic component can vary significantly between people and skin path length between the electrodes; and should thus be filtered out to obtain the phasic component from which sleep cycle information can be gathered. Based on the characteristics of the tonic component, a high-pass filter of 0.016 Hz is appropriate (28).

## **2. SLEEP DETECTION RESEARCH**

---

Digitising the measured skin conductance requires converting the measured current to a voltage and sampling discretely. A sample rate of 15-20Hz is sufficient, but the signal should be further low pass filtered at less than the Nyquist rate to capture the EDA signal but filter noise and artefacts (37). Low pass filters that operate down to 5Hz are sufficient (28).

### **2.8.2 Electrode Placement**

Traditionally electrode placement has been confined to the palm of the hand, and the fingers. Both of these locations are highly susceptible to body motion artefacts as the hands are commonly used for manipulating objects, which can interfere with measurements. Often, the non-dominant hand is used, because it tends to have less cuts and calluses which can effect EDA, and has the added benefit of leaving the dominant hand free for other tasks. There has been no definitive evidence obtained to show a difference in recordings obtained from either hand (5). There is no general standard for electrode placement for electrodermal sites, as the main aim is to maintain a constant contact area, which varies depending on implementation. EDA monitoring has been effectively implemented with electrodes placed on the ventral side of the distal forearms (25), as shown in figure 2.7.

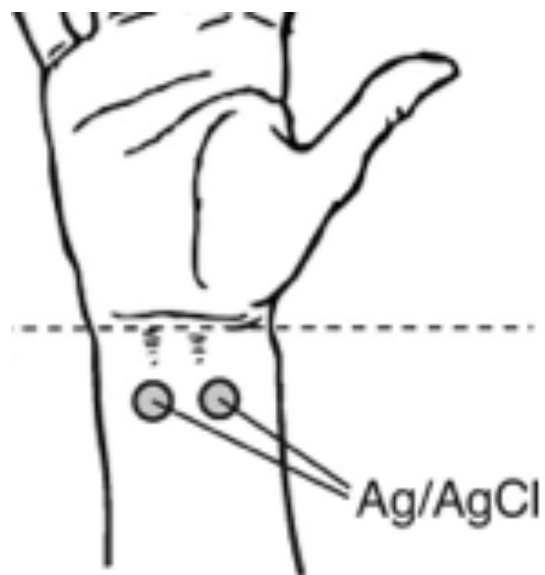


**Figure 2.7: Electrode Placement** - Wrist placement of electrodes for EDA measurements (25).

It is important to minimise the bias potential between the pair of electrodes, and prevent polarisation as a result of electrical current interactions; both of which can be achieved by using reversible silver/silver chloride disk electrodes of diameter between 8 to 11mm (28).

A gel is often required for use with electrodes. With EKG, EEG or EMG the gel should be of high conductivity to help propagate electrical signals to the electrode. In contrast, EDA measurements require minimal interactions between the skin and the electrode. Hence, an isotonic gel (same ion concentration as sweat) is commonly used. However, there have been successful implementations of EDA monitoring without the use of any gel (25). There is no definitive evidence that pre-treatment to remove dirt, oils and existing sweat from the skin is necessary to achieve good results (28).

## 2.9 Summary

The two main sleep pattern detection technologies are polysomnography and actigraphy, both of which are typically used for medical diagnosis of sleep disorders. Several other unique detection methods were discussed in this chapter, including electrodermal activity correlation, load cell analysis, and actigraphic machine learning algorithms.

It is made apparent that the human physiology changes relatively predictably during sleep, and that these changes can, and have been detected to produce information relating to sleeping patterns. Research relating to changes in motion, skin temperature and heart rate during sleep show clear features that can, and have been correlated with particular sleep stages.

## **2. SLEEP DETECTION RESEARCH**

---

# Chapter 3

# Design and Implementation

## 3.1 Introduction

The deliverables of the automated waker system have several critical aspects that are required in its design. The system must utilise multiple sensors which require contact, or a close proximity to the user (i.e. worn attached to the body in some way). As such, an unobtrusive, wireless and small profile is required to minimise the user's physical awareness of the system and prevent the inhibition of natural behaviours.

The design of wireless devices necessitates several considerations, as limitations arise with respect to communication range, the possibility of signal interference and perhaps most considerably - the powering methodology. Consequently, the processing capabilities of wireless devices often need to be limited to reduce power consumption. The analysis of sensory data to determine sleep patterns is a relatively intense process however, and to overcome these limitations the system is comprised of two main components: a sensor module and a computer module.

The sensor module focuses on the collection of raw data, and the subsequent transmission of said data to the computer module. The storage, processing and analysis of the data is performed by the computer module, which consists of an application on a personal computer that utilises its inbuilt hardware. Such a system configuration minimises the processing and powering requirements of the wireless components required to be in close proximity to the user.

Figure 3.2 portrays the high level overview of the system. The sensors used to detect the user's current stage of sleep are a pulse oximeter, accelerometer and temperature

### **3. DESIGN AND IMPLEMENTATION**

---

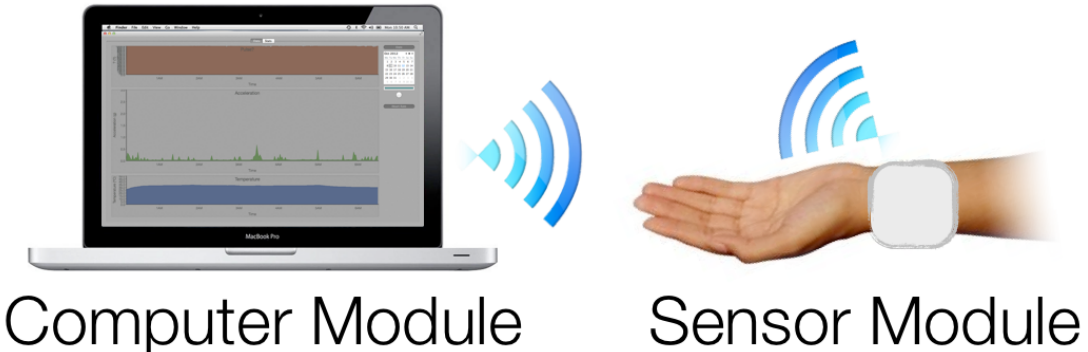


**Figure 3.1: Modular Design** - Wireless connection between a sensor and computer module

sensor; while the actuators that influence the user's sleep patterns to induce a more natural awakening are a vibration motor, screen (light) and speaker (sound).

This chapter will discuss the design considerations associated with the system and each module, relating especially to the:

- requirements of the sensors to supply adequate data for analysis
- design of the sensor modules hardware and enclosure
- aspects of both modules involved in the awakening process (i.e. vibration motor)
- requirements of the computer for storage and processing

## **3.2 Sensor Module**

The purpose of the sensor module is to gather meaningful data relating to the wearer's sleep patterns and current level of wakefulness. The design of this module consists primarily of three sensors - an accelerometer (section 3.2.1), temperature sensor (section 3.2.2) and a pulse sensor (section 3.2.3), which gather this data. The module also requires wireless communication hardware and a microcontroller to manage the sensory data.

The entire module has been designed to be worn on the user's wrist, inside an elastic sweatband-like material as seen in figure 3.3, and discussed in section 3.2.8.

This section will discuss and justify these design choices with specific detail to individual sensors and other relevant components.

### 3.2 Sensor Module

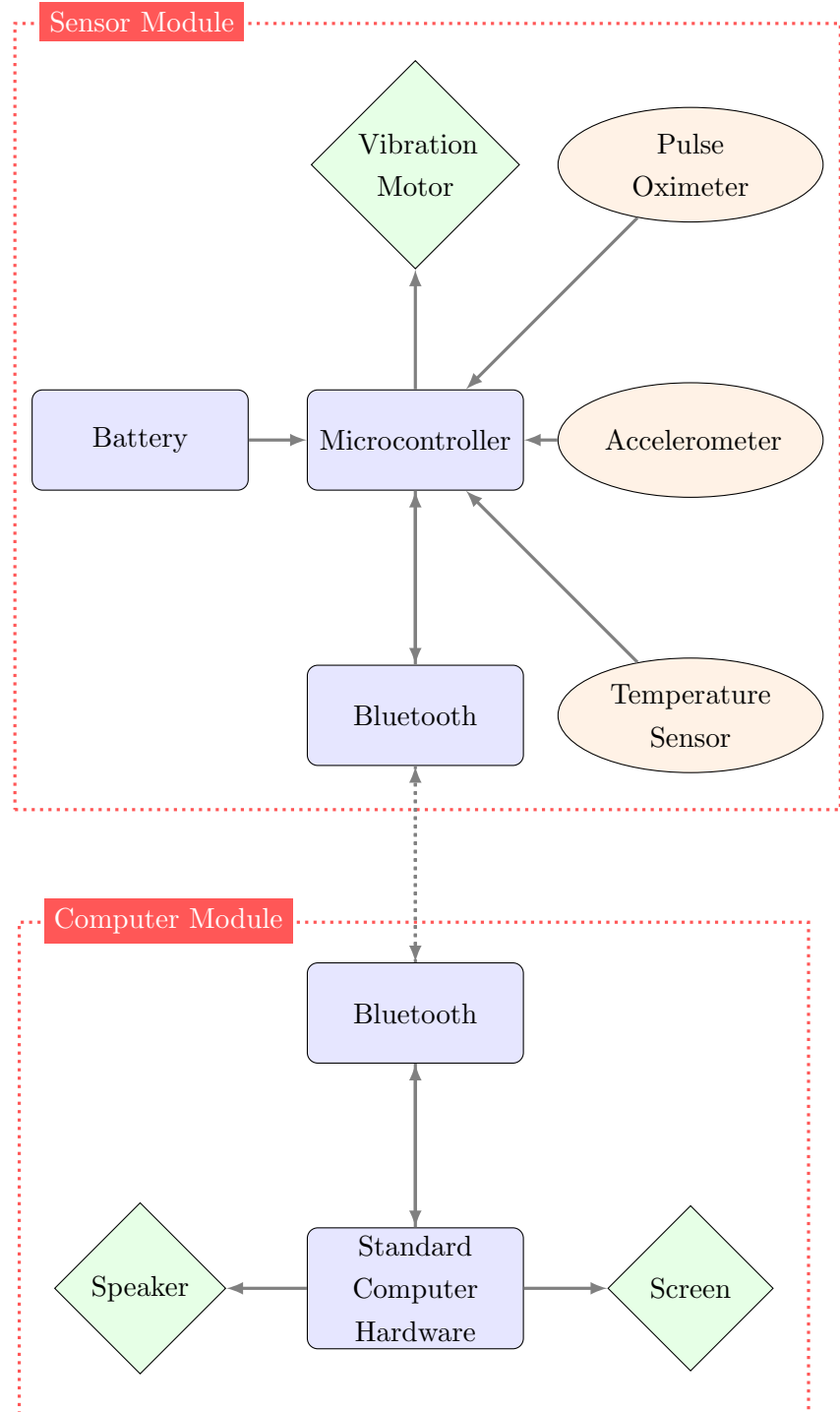


**Figure 3.2: Design Overview** - Block Diagram. Arrows show primary communication direction between sensors (orange), actuators (green) and other components (blue).

### **3. DESIGN AND IMPLEMENTATION**

---



**Figure 3.3: Wrist Enclosure** - Sensor module contained and worn within a wristband.

#### **3.2.1 Accelerometer**

One of the most revealing physiological changes during the sleep cycle is a human's motion behaviours. An accelerometer can be used to detect motions and correlated to specific stages of sleep as discussed in section 2.4. The properties of our motion dictate the necessary capabilities required of the accelerometer used. These requirements are:

- sample rate sufficient to detect motions that rarely exceed 5Hz
- sensitive enough to detect changes in acceleration of the magnitude of 50mg
- measurement range sufficient to detect significant motions exceeding 2g's

The ADXL345 is a triple axis accelerometer that meets these requirements, and has several other useful characteristics and features such as low power operation and inactivity detection. The following are some relevant specifications of this accelerometer:

- up to 3200Hz sample rate
- 4mg sensitivity (13-bit resolution data)
- up to  $\pm 16\text{g}$  measurement range
- low power operation, as low as  $40\mu\text{A}$  in measurement mode and  $0.1\mu\text{A}$  in standby

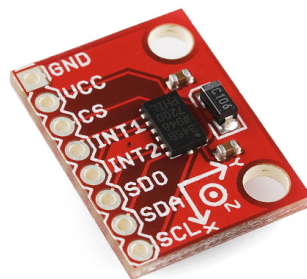


**Figure 3.4: ADXL345 Accelerometer - Breakout Board**

- operable within  $-40^{\circ}\text{C}$  to  $+85^{\circ}\text{C}$  temperature range

Like most components in this module, this accelerometer is available manufactured on a breakout board - designed for prototyping. The IC's pins are more easily accessible for development and testing with, for example, a breadboard or protoboard; and the two standoff holes allow for secure attachment.

The mounting location of the IC in the PCB, and of the PCB itself are quite critical. If the IC is insufficiently supported the accelerometer may report large apparent measurement errors due to undamped PCB vibrations. In this implementation, the frequency of these vibration's was limited to be insignificant compared to the sensor's mechanical resonant frequency. This was achieved by ensuring the breakout board was secured using the standoffs as points of attachment, supplemented with a silicone bond to the sensor module's enclosure (described in more detail in section 3.2.8).

One disadvantage of using the accelerometer on a breakout board is that its size is larger than required. Its dimensions are  $21\text{mm} \times 16\text{mm} \times 2\text{mm}$ , compared with the IC's dimensions of  $3\text{mm} \times 5\text{mm} \times 1\text{mm}$ . However, the size of the breakout board is still small enough to fit in a reasonably sized enclosure (discussed in section 3.2.8). In future work, the device could be implemented significantly miniaturised by manufacturing a single PCB incorporating each component.

Three axes of acceleration should be monitored as the accelerometer can not be guaranteed to be at any particular orientation due to the range of configurations of the human body and wrist. In this system's implementation, only the magnitude of

### **3. DESIGN AND IMPLEMENTATION**

---

acceleration above 0g's (after removing the gravity offset) is required to differentiate motions sufficiently. This process is discuss in section 4.2, particularly with respect to equation (4.2).

This assumes that the accelerometer will experience only the acceleration due to gravity for significant amounts of time; additional accelerations will mask, and even affect the human's sleep motions. Hence, this aspect of the system will not function correctly if used within say, a moving vehicle. The user should be made aware of this limitation, and the device should still wake the user within the user specified timeframe. The current implementation achieves this, and in future work the detection of unexpected motion could be categorised or even filtered out to allow full operational quality.

A similar limitation for this system is encountered in the case where the user's arm/wrist motion is inhibited. This could occur, for example, if the user's torso rolls on top of their wrist. It would be beneficial to test what can be interpreted from data collected in such a situation, as there is a possibility that sleep cycles could still be determined accurately, and this is recommended for future implementation.

The accelerometer has been configured to sample at 12.5Hz, which corresponds to a typical current flow of  $55\mu\text{A}$ . The maximum expected motion frequency is 5Hz, as previously mentioned, and hence the minimum sample rate to prevent aliasing and misinterpretation of motion frequencies is 10Hz (as determined through Nyquist's Theorem).

The acceleration measurement range can be selected as  $\pm 2\text{g}$ ,  $\pm 4\text{g}$ ,  $\pm 8\text{g}$  or  $\pm 16\text{g}$ . In full resolution mode, the sensitivity is  $4\text{mg}/\text{LSB}$  for each selectable measurement range, and hence there is no benefit for using the  $\pm 2\text{g}$  setting than for the  $\pm 16\text{g}$ , at least with respect to measurement resolution. For this reason, the  $\pm 16\text{g}$  setting is used enabling the nonessential detection of rare high accelerations that otherwise might be truncated in other settings.

Communication between the accelerometer IC and the microcontroller is performed using the I<sup>2</sup>C protocol - described in greater detail in section 3.2.4. Through this connection, the accelerometer is configured, and is queried for data.

There are three inbuilt data collection modes; stream mode being the one of most use for this system. In this mode, the data is stored in a buffer capable of reserving 33 acceleration samples (in bytes this is: 3 axes  $\times$  2 bytes per sample  $\times$  33 samples = 396

bytes of data storage). This buffer is a FIFO buffer, meaning the first data recorded is the first to be obtained from a query. Thus, the oldest data is acquired first and the newer samples are stored for subsequent queries. Should the buffer be filled, the oldest data is overwritten.

This buffer mode means that each set of data read from the accelerometer is in the correct sequence, where the time between samples can be accurately assumed based from the configured sample rate. This assumption is void if the buffer is filled and old data is overwritten, in which case it is necessary for the microcontroller to be made aware of this overrun to ensure subsequent reads of data can be accurately timestamped. Fortunately, the accelerometer has two configurable interrupt pins capable of reporting an overrun incident to the microcontroller. These pins are connected directly to two of the microcontroller's pins, situated on the pin change interrupt port (a PORTB alternate function). When the accelerometer signals, the microcontroller can very quickly handle the cause of the interrupt. The interrupt pins can not only be configured to signal when the sample buffer overruns, but also when:

- data is available (i.e. when the buffer is not empty) - used to efficiently query the accelerometer for data only when it is available.
- a period of inactivity occurs - after a specifiable time interval (implemented as 180 seconds) and when the acceleration does not exceed a change threshold during this time, an interrupt is triggered and the microcontroller considers entering sleep mode (described in further detail in section 3.2.4).
- activity occurs - when acceleration exceeds a threshold the accelerometer signals the microcontroller. This interrupt is the only one that can be configured to work when the accelerometer is in sleep AND measurement mode. In this mode, the accelerometer uses less power, doesn't store data in the stream buffer, and drops the sample rate to 8Hz. This feature is crucial for waking the system from sleep to capture relatively rare motions - especially when the user is experiencing deep sleep.

Accelerometers often have inherent offsets and gain errors, which in this application would interfere with components of the processing and analysis (section 4.2). Hence

### 3. DESIGN AND IMPLEMENTATION

---

Axis	x	y	z
+	1.0569	1.0608	1.0569
-	-0.975	-0.9828	-0.936

**Table 3.1: Accelerometer Calibration** - Acceleration (g) for each axis when aligned with gravity. Initial offset: 0. Initial gain:  $3.9 \times 10^{-3}$ .

the calibration of the accelerometer is necessary, and was performed through two processes. The first being an inbuilt self-test function, where the accelerometer applies an electromagnetic force on itself to simulate acceleration. The data output should be within given thresholds to suggest sufficient linearity and proper functionality.

The second calibration process is performed to determine any offset accelerations and scaling errors. This process involves sequentially aligning each axis of the accelerometer with the direction of gravity, and recording the maximum value in that axis (while ensuring the accelerometer is stationary). This process is repeated for each axis, both in the positive and negative directions, totalling 6 average maximum measurements, as shown in table 3.1.

The initial gain was determined from the accelerometer's typical sensitivity of 3.9mg/LSB, and used primarily to scale the accelerometer data to have meaningful (albeit possibly inaccurate) units before calibration (g's). Under the assumption that gravity was acting typically at the location of testing, the maximum values for each axis should have been 1g. The measurements in table 3.1 portray the necessity for calibration, where there is a positive offset inherent in each axis of the accelerometer. In comparison, the initial estimated gain of  $3.9 \times 10^{-3}$  seems relatively accurate as each maximum is close to 1g. These measurements are the averages of three repeated calibrations, for increased accuracy.

The offsets and gains for each axis can be determined using the equations (3.1) and (3.2) respectively:

$$o_k = \frac{a_{k+} + a_{k-}}{2} \quad (3.1)$$

$$g_k = \frac{a_{k+} - a_{k-}}{2} \quad (3.2)$$

Where  $k = x, y, z$ ;  $a_{k\pm}$  are the maximum positive and negative measurements for each axis (those shown in table 3.1);  $o_k$  and  $g_k$  are the offsets and gains, respectively, for

Axis	x	y	z
Offset (mg)	-40.95	-39	-60.45
Gain ( $\times 10^{-3}$ )	3.8388	3.8168	3.9139

**Table 3.2: Accelerometer Coefficients** - Offset and gain applied to each accelerometer axis.

each axis. The calculated offsets and gains must be subtracted and divided respectively, from the initial coefficients. These values are portrayed in table 3.2.

#### 3.2.2 Temperature Sensor

A human's body temperature varies between levels of wakefulness, as discussed in section 2.5. This relationship can be correlated with the data obtained from a temperature sensor, ergo its inclusion in the design. Temperature sensors are also cheap, low power, and require little data processing - substantiating the use of this type of sensor in this module.

In this design, skin temperature is measured instead of body temperature, due to the more accessible measurement locations required. As discussed in section 2.5, one of the issues with measuring skin temperature is that it can be affected more significantly by factors external to the body and its circadian rhythm, meaning artefacts may be present in the data, e.g. from the shifting of the sensor from beneath bed covers, into a cooler/warmer environment. In this situation the skin temperature being measured is likely to change significantly while the core body temperature remains the same.

To help counteract these changes, the computer module also gathers temperature data from one of its many internal temperature sensors (specifically, one that monitors the enclosure temperature) to compare and analyse the measured skin temperature.

There are several specifications required of the sensor module's temperature sensor, in order for it to acquire data that is relatable to the sleep cycle. The sensor should have:

- sufficient measurement range - skin temperature can range from 27°C to 36°C
- high resolution - at least 0.1°C (35)
- fast response to temperature change - low thermal resistance

### **3. DESIGN AND IMPLEMENTATION**

---

The TMP102 temperature sensor is encapsulated entirely in a small IC and requires no external components. This chip meets the above requirements, having the following specifications:

- measurement range of -40°C to +125°C
- temperature resolution of 0.0625°C
- typical accuracy of 0.5°C
- low thermal resistance of 260°C/W
- low power - 10 $\mu$ A while active, 1 $\mu$ A in sleep mode

Like the ADXL345 Accelerometer, the TMP102 Temperature Sensor is readily available on a breakout board, presenting the same advantages.

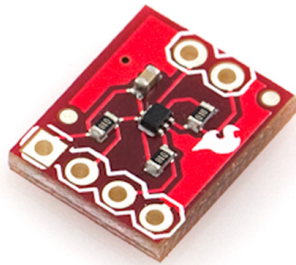


**Figure 3.5: TMP102 Temperature Sensor - Breakout Board**

While this sensor easily meets the requirements, it requires a relatively complex mounting procedure to allow it to be in contact with human skin. Because of the exposed electrical components on the breakout board, contact with sweat or moisture could cause corrosion and potentially short circuiting. The mounting procedure is described in section 3.2.8. In summary, the circuitry is enclosed in a thermally conductive silicone to prevent corrosion, short circuiting, and unwanted air flow, as well as to allow significant heat transfer. The silicone has a high thermal conductivity of 1.58 W/mK (that is, a resistivity of 633°C/W). While more conductive to heat than most silicones

and alternatives, it is still of higher resistance than the temperature sensor package itself, so this substance is applied as a thin layer over the exposed electronics to minimise thermal resistance. The silicone can be shaped to allow for a smooth surface to be in contact with the skin, reducing heat leakage to and from the environment and improving the validity of the temperature measured.

Variations in skin temperature occur over relatively long time periods, allowing for a low sample rate to be used to accurately portray changes in skin temperature over time. In this application, a sample rate of 2Hz was used.

Communication with the microcontroller is performed using I<sup>2</sup>C, with the same communication lines as for the accelerometer, limiting required components and wires. The details of the protocol are described in section 3.2.4. Through this connection, the temperature sensor is configured, and is queried for data.

### 3.2.3 Pulse Oximeter

Measuring the user's heart rate is an important part of this design, as the recorded data can be correlated to different stages of sleep with knowledge of the expected behaviours discussed in section 2.6.

Measuring heart rate on the wrist is performed with reflectance pulse oximetry, because of its minimal hardware and powering requirements when compared to other methods. As discussed in section 2.7, an ECG requires multiple electrodes placed at different locations on the body, and absorption based oximetry senses the degree of light passed through thin flesh - both of which are unsuitable for wrist based heart rate detection.

Pulse oximetry doesn't measure heart rate directly, but rather measures the oxygen content of the blood, which oscillates with each beat of the heart (and can experience other lower frequency changes). Hence the data processing introduced in section 4.4 is required to determine the heart rate.

With reflectance based oximetry, the LED and photodiode are situated next to each other so that light emitted by the LED that is reflected from the user's skin (and blood beneath) can be detected by the photodiode.

The sensor used to detect this variation in blood oxygen content consists of a green, super bright reverse mount LED from Kingbright (AM2520ZGC09) and an ambient light sensor from Avago (APDS-9008). This sensor (available from pulsesensor.com) is

### **3. DESIGN AND IMPLEMENTATION**

---

manufactured with some additional basic circuitry - primarily a low pass filter (cutoff 340Hz) and an operational amplifier. A bandpass filter matched to the maximum and minimum heart rate frequencies expected would have been more appropriate, however this was implemented in software.

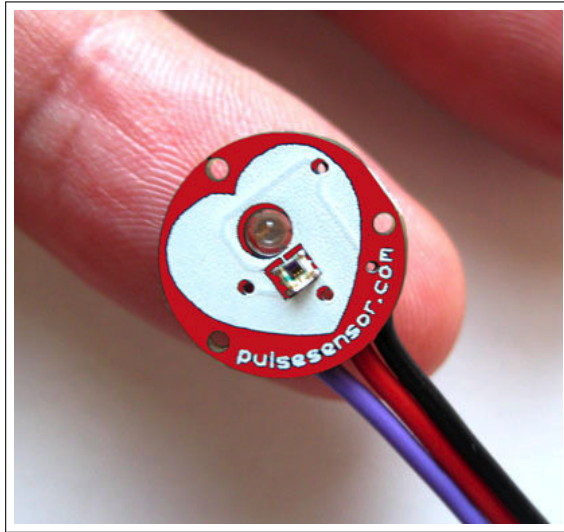


**Figure 3.6: Pulse Oximeter** - The LED (round) and photodiode (rectangular) components are visible in the centre. The red and black wires are 3.3V and ground respectively, the purple wire is the analogue signal output.

For pulse oximetry, a green LED is a rather unconventional colour, as blood absorbs the lower frequency red light to a higher degree, however the choice is justified by the ratio of brightness of the LED to the power it consumes - which is higher than other red LEDs around the same power range. The LED's peak intensity wavelength is 515nm, which the photodiode matches with in order to maximise signal detection and efficiency.

Like the temperature sensor, the pulse oximeter requires secure contact with the skin, preferably with reasonably high blood flow beneath (such as most areas on the underside of the wrist). Consequently, the oximeter circuitry must also be protected from moisture. Unlike the temperature sensor, the oximeter can't be covered in silicone because light must pass through. To overcome this limitation, a thin transparent plastic cover was used, and then the sensor was embedded in silicone taking care to only cover the edges of the PCB to secure it in place and protect the underside from moisture. This ensures the sensor's circuitry is moisture resistant, without impeding its operation.

The usage of the sensor to collect the raw data is remarkably simple, requiring only three wires: two for powering the sensor, and one that outputs an analogue signal (as shown in figure 3.6). There is no internal configuration, so unlike the other components in the system, the pulse sensor can simply be turned off when the system enters ‘sleep’ mode.

The voltage range of the analogue signal is between Vcc (3.3V) and ground (0V) - dependant on the photodiode’s measured light intensity. For transmission and processing, this analogue signal must be converted to a digital form, which is discussed in section 3.2.4. The sensor runs at 2.5mA, even though the LED is rated at 20mA. Because the LED is very bright when at full power, this limited current is sufficient for pulse oximetry.

Determining the necessary sample rate is primarily dictated by the maximum frequency signal that should be measured, and post-processing that is required. The system is designed with a maximum signal frequency equivalent to 300 heart beats per minute ( $= \frac{300bbm}{60s/min} = 5Hz$ ), which should be more than anyone experiences during normal sleep. The Nyquist Rate is thus 10Hz (minimum sampling rate), however the post-processing that should be performed (specifically, filtering - as discussed in section 4.4) will produce better results with higher sample rates. A compromise between these factors and ADC timing concerns resulted in the use of 50Hz as the sample rate.

#### 3.2.4 Microcontroller

The sensor module is useless if the accelerometer, temperature sensor and pulse sensor cannot communicate the measurements they acquire. These sensors could be wired directly to a purpose built IC that relays the sensory data directly to the wireless communication circuitry, but this would be difficult, impractical and un-customisable. Utilising a microcontroller to perform this relay of data is quite necessary, as a microcontroller can also perform operations to manage the functioning of the entire sensor module and handle detected events (e.g. accelerometer inactivity or a command sent from the computer module).

The main specification requirements for the microcontroller are:

- small size - to minimise required enclosure size

### **3. DESIGN AND IMPLEMENTATION**

---

- ease of development - must be easily reprogrammed, and incorporate most - if not all, other less significant required components
- reasonable tradeoff between clock speed and power usage
- I<sup>2</sup>C - for communication with accelerometer and temperature sensor
- ADC - for interpretation of the pulse sensor's analogue signal output
- UART - communication with wireless communication component.

One option that meets these requirements is the Teensy 2.0 Development Board, featuring an ATMEGA32U4 microprocessor, 32kB of flash memory, 2.5kB of RAM, 25 I/O pins - 12 of which can be configured as analog input pins, I<sup>2</sup>C and UART. It measures in at a small 17.8mm × 30.5mm profile - suitable for use in the sensor module. All programming is done simply via the USB port.

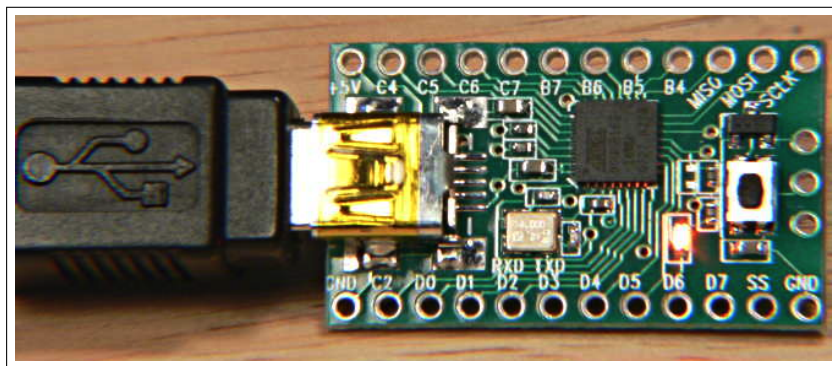


**Figure 3.7: Teensy 2.0 Development Board - μUSB cable attached for loading code.**

While the microcontroller must relay sensory data to the computer module, it must also perform several other operations, of which an overview is depicted in figure 3.8.

The initialisation stage configures each of the sensors and other components, as well as certain aspects of the microcontroller itself, like the clock speed and the I<sup>2</sup>C module. The microcontroller then enters sleep mode and waits until the computer module confirms the wireless connection. Before a connection is made, the microcontroller could start collecting data and store it in onboard memory, and then send the collected data upon connection with the computer module - but due to the limited memory available it's likely to be filled quickly making the storage process redundant.

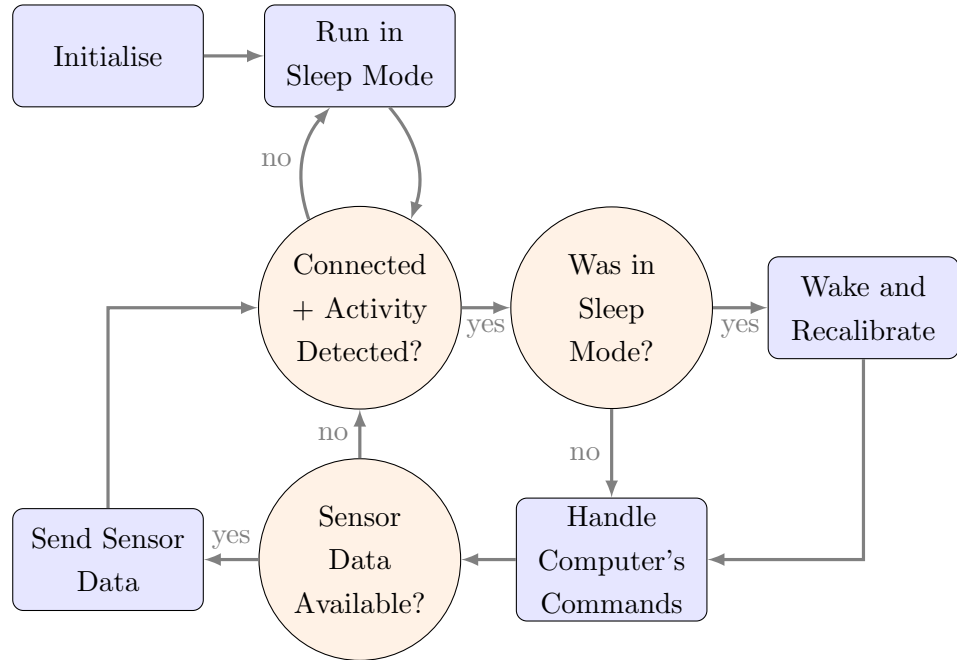


**Figure 3.8: Microcontroller Operation - Simplified Flow Chart**

Once wirelessly connected to the computer module, the microcontroller must wake itself and each of the sensors, as well as recalibrate the timing to ensure valid timestamps are sent between the computer module and itself. The next step is to handle any received commands from the computer module (these commands are received in an interrupt and stored for processing in the main loop). These commands include to enter sleep mode, or to vibrate to wake the user. Finally, the sensory data is obtained from each sensor if available (i.e. if enough time has passed for a new sample to be obtained, which is different for each sensor).

The microcontroller is pre-scaled to run at 1MHz for lower power consumption, more specifically the Teensy uses  $\approx 2\text{mA}$  (at 3.3V) when running at 100% (no idling or sleeping). In sleep mode, the microcontroller runs at less than  $40\mu\text{A}$ , a key feature for conserving battery power. The 1MHz clock speed was determined through iterative tests to find the minimum speed required that still allows sufficient sensor sampling, reasonable communication speeds and overall correct functionality.

The communication between the accelerometer and temperature sensor with the microcontroller is performed using the I<sup>2</sup>C protocol. This communication method can send and receive data on a single wire, with a second wire responsible for timing the

### 3. DESIGN AND IMPLEMENTATION

---

data transmission and reception as depicted in figure 3.9. I<sup>2</sup>C represents a high speed, low power, robust communication technology suitable for use with multiple compatible IC's.

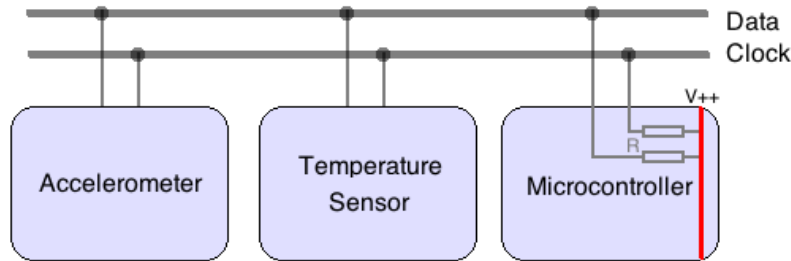


**Figure 3.9: Microcontroller - Sensor Communication - I<sup>2</sup>C**

Speeds up to 3.4MHz can be obtained with this microcontroller when its clock speed is sufficient. However, such high speeds are excessive for this application and result in undesirably high power usage. Hence, a speed of 12.5kHz was chosen for a couple of reasons. The first is that such a low speed allows the use of the internal 50kΩ pull-up resistors without resulting in a significant I<sup>2</sup>C clock/data rise time. The second is that each component communicating via the I<sup>2</sup>C bus uses less power.

Unlike the accelerometer and temperature sensor, the pulse oximeter outputs an analogue signal which must be converted to its digital equivalent in order to be recorded. This is performed using the microcontroller's inbuilt analogue to digital converter (ADC), which has the following relevant features:

- 10bit resolution
- ±2 LSB accuracy
- ground - Vcc voltage range
- auto trigger timing mode

This resolution corresponds to 3.22mV/LSB ( $= \frac{3.3V}{2^{10}}$ ), where a typical variation in signal voltage due to heart beat was specified to be around 60mV (using the same model of sensor, measured on the fingertip). This is sufficient to discretise the signal without overly affecting the waveform, however it may be determined that the typical

signal voltage variation as measured on the wrist is smaller, in which case an additional amplifier and bandbass filter (matched to the minimum and maximum heart rate frequencies expected) may be required.

The measurement range of the ADC is specified by a reference voltage applied. In this case, the sensor operates from ground (0V) to Vcc (3.3V), which corresponds to the maximum (and default) range the ADC can operate.

As discussed in section 3.2.3, the pulse oximeter signal should be sampled at 50Hz. To achieve this as accurately as possible, a 16bit prescaled timer is utilised with a compare match interrupt at 0.02 seconds ( $\frac{1}{50\text{Hz}}$ ) to trigger an ADC conversion.

One further consideration for the pulse oximeter is its control with respect to powering and sleeping. The sensor can only be turned on and off by adjusting its supplied voltage. To do this, the sensor's positive voltage (Vcc) wire is connected to an output pin of the microcontroller. As such, the microcontroller can simply drive that pin high to turn on the sensor, and low to turn it off (i.e. sleep). The microcontroller's current supply is limited to 40mA for each output pin, which is easily sufficient to power the oximeter which runs at 2.5mA.

#### 3.2.5 Wireless Communication

The sensor module must communicate wirelessly with the computer module, as wired communication would likely interfere with the user's sleep behaviour by restricting movement and entangling undesirably. There are various forms of wireless communication that modern computers utilise, primarily wi-fi and bluetooth, but also several other proprietary technologies. Other communication technologies are also available where a device can be attached to the computer to allow communication (e.g. an XBee dongle, or the Nordic USB ANT Stick introduced below).

As with every component in the sensor module, one of the most desirable characteristics of this communication is low power requirements. Additionally, it is very important that the connection is robust, with a reasonable communication range appropriate for use within the room of a house (at the least).

The Nordic nRF24AP1 and accompanying Nordic USB ANT Stick are a very low power option that was initially used in this system. However, due to their low power signal and particular communication protocol the range for which they operated successfully was less than a metre, due primarily to interference with external wi-fi signals

### **3. DESIGN AND IMPLEMENTATION**

---

in the environment. This insufficiency was too significant an issue to the operation of the system that a more common alternative was used: bluetooth. Bluetooth is an open wireless technology standard for transmitting and receiving data over short distances. It utilises short wavelength radio in the 2.4-2.48GHz band, using high levels of security, and capable of synchronisation between multiple connected devices. The components required for operation are typically small and operate with low power demands. Most modern computers contain a bluetooth device capable of managing several bluetooth connections at once. The computer module used (a mid-2009 MacBook Pro) has this capability, and thus an external bluetooth USB dongle (or the like) was not required.

The bluetooth component used within the sensor module of this thesis is the BlueSMiRF Silver, which utilises the RN-42 module. The BlueSMiRF is capable of data transfer at 1200bps to 921kbps, with the typical communication range of 18m. To the computer (after being handled by the bluetooth manager), the bluetooth connection appears as a simple serial port. The BlueSMiRF's power consumption is one of the most considerable in the sensor module, with 45mA during data transfer, 25mA connected but idle, and  $26\mu\text{A}$  during deep sleep.

Several configurable settings can be used to reduce power consumption, and these were utilised to a great extent:

- inquiry scan window - during this time the device can be discovered by other bluetooth devices in range. This is configured to be at the minimum 1% duty cycle, where the computer module picks up the strain by looking for devices at a higher frequency.
- page scan window - during this time the device can be connected with. Again, the minimum of 1% duty cycle is used, and the computer attempts to connect more often.
- baud rate - set to 9800bps
- low power connect mode - when not connected, enters deep sleep for 10 seconds, every 20 seconds. During this time the device can not be connected to or even discovered.
- sniff mode - enters low power mode when no data transfer is detected, drawing 0.3mA. Set to sniff for data every second.

Data	Acceleration	Temperature	Pulse
Bytes	6	2	2
Rate (Hz)	12.5	0.5	50
bps	75	1	100
Total bps	176		

**Table 3.3: Bluetooth Data Rate - Bytes Per Second (bps)**

The expected amount of data to be transmitted when operating is portrayed in table 3.3, based on the settings described in each sensor's section of this chapter. This is important when determining the power consumption, which can be approximated using equation (3.3), where D is the transmission duty cycle, and P is the average power used (45mA is used when transmitting, 0.3mA otherwise).

$$D = \frac{176}{9800} \approx 1.8\% \quad (3.3)$$

$$P = 45mA \times D + 0.3mA \times (1 - D) \approx 1.1mA$$

The BlueSMiRF breakout board itself has a profile that is slightly larger than the other sensor module components, being 45mm × 16.6mm × 3.9mm - shown in figure 3.10. The antenna is of a compact form and can be seen in the figure as the trace within the blue PCB section. Larger antennae can be attached for increased range and signal strength, but at the expense of increased power consumption, weight and size - hence the reason for its exclusion.

#### 3.2.6 Power

The sensor module's components that draw the most significant power have now been introduced, and an estimate of the module's power requirements can be deduced from each components specifications and configuration.

Each component is designed to operate at 3.3V, with the exception that the microcontroller runs at 5V by default. The Teensy microcontroller can be used at 3.3V with the simple addition of a MCP1825S Voltage Regulator to its underside, as depicted in figure 3.11. The process involves soldering the regulator pins onto the large ground pad (right of regulator), and the smaller  $V_{in}$ ,  $V_{out}$ , and ground pads (left of regulator);

### 3. DESIGN AND IMPLEMENTATION

---



**Figure 3.10:** Bluetooth Module - BlueSMiRF Silver

followed by the solder connection of the 3.3V pad and the middle pad that powers the microcontroller (the 5V trace must be cut as well).



**Figure 3.11:** Voltage Regulator - MCP1825S Regulator attached to Teensy 2.0.

The addition of the MCP1825S Voltage Regulator is actually necessary for another reason - almost every kind of battery will experience a voltage drop as it is drained. The voltage regulator does exactly that, maintaining a constant 3.3V output. It operates with input voltages ranging from 2.1V to 6V meaning the module will be able to operate correctly for a longer period of the batteries lifecycle. The regulator can easily cope with the power load, with a maximum output current of 0.5A, and only  $120\mu\text{A}$  needs

### 3.2 Sensor Module

---

Component	Current ( $\mu$ A)		Power (mW)	
	Operating	Sleep Mode	100% Duty	50% Duty
Accelerometer	55	0.1	0.182	0.091
Temperature Sensor	10	1	0.033	0.0182
Pulse Sensor	2500	0	8.25	4.125
Microcontroller	2000	40	6.6	3.366
Bluetooth	1100	26	3.63	1.86
Regulator	120	120	0.396	0.396
Total	5785	187.1	19.01	9.854

**Table 3.4: Power Breakdown** - Component's Power Usage

to be supplied for operation.

Before a battery can be chosen for powering the sensor module, its capacity requirements must be determined based on the power requirements for each component within the sensor module. Table 3.4 summarises this power requirement where the operating and sleep mode currents for each component have been discussed in respective sections.

One final factor in power consumption is the effect of the reverse voltage protection circuitry which is important to prevent damage to the system if the battery is inserted backwards. This is achieved with a IN5820 3A Schottky barrier rectifier diode, which was chosen primarily for its low forward voltage drop of 0.2V. The voltage regulator still maintains the system voltage at 3.3V, but this drop across the diode introduces a power loss proportional to the current drawn through it ( $0.2V \times xA$ ), increasing the power used for 100% and 50% duty cycles from 19.01mW and 9.854mW, to 20.17mW and 10.45mW respectively.

Ideally, a battery with enough capacity to run the sensor module at 100% duty (i.e. never enters sleep mode) for a whole night would be used. Such a battery would require a minimum of  $20.17\text{mW} \times 10 \text{ hours} = 201.7\text{mWh}$ .

A battery of sufficient capacity at a small size is the CR2450 coin cell category. Rechargeable batteries in this category were used. They have capacities of 396mWh (3.6V and 110mAh), which meets this criteria. They can be recharged with appropriate coin cell battery recharger units, which is advantageous in this system where the batteries will likely require recharging every 1-2 days.

### **3. DESIGN AND IMPLEMENTATION**

---

The breakout board shown in figure 3.12 allows for secure attachment of a CR2450 battery within the device, and simplifies the connection to the voltage regulator.

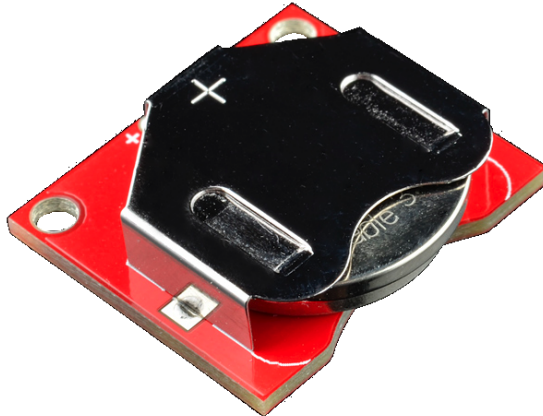


**Figure 3.12: CR2450 Battery - Breakout Board**

The regulated voltage output available from the microcontroller (via the voltage regulator) powers each of the other components in the sensor module. Due to the nature of some of these components, transients can be present in the power lines which degrade the accuracy of the measurements obtained from the sensors. Two  $0.1\mu\text{F}$  capacitors are placed between the power and ground lines to mitigate these transients, and both the ADXL345 accelerometer and TMP102 temperature sensor have inbuilt decoupling capacitors.

#### **3.2.7 Vibration Motor**

One of the stimuli of the systems awakening process is vibration (touch), which requires a source of such vibration to be in contact with the user's body. Consequently, a vibration motor is incorporated into the sensor module.

The Precision Microdrives 310-10 Shaftless Button Type Vibration Motor, of 10mm diameter and 3.4mm height; weighing just 1.2 grams, it induces quite a significant vibration for its size. It operates between 2.5-3.8V, with a rated current of 75mA. The motor can be seen in figure 3.13. The underside of the motor comes with an adhesive for a more secure attachment to the enclosure.

It must be controlled by the microcontroller if it is to be turned on and off at dynamically determined times, however, a microcontroller output pin can only supply

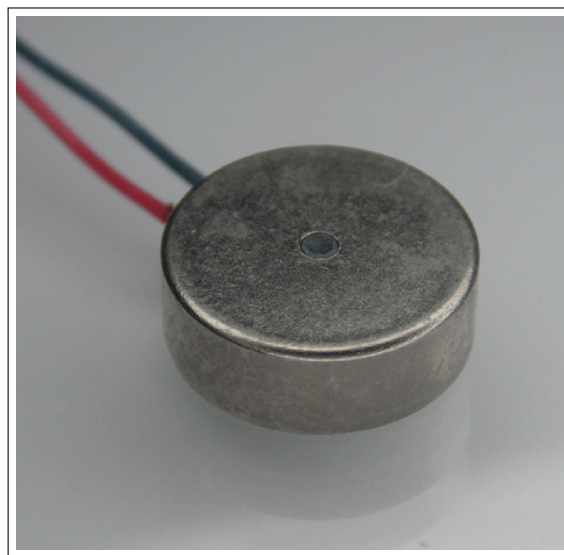


**Figure 3.13: Vibration Motor** - small but powerful

a maximum of 40mA. Hence, the current limiting circuit in figure 3.14 is used. The  $47\Omega$  resistor reduces the current drawn from the microcontroller to motor, and the diode prevents significant back EMF current that could damage the microcontroller.

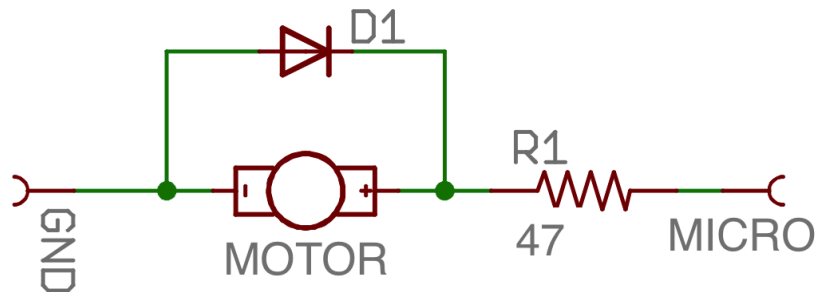


**Figure 3.14: Vibration Motor Control Circuit** - Microcontroller Protection

While this current seems high relative to that required by other components, the vibration motor is only on for very small time periods per day. For example, typical usage would be for 20 seconds, with the motor pulsing on and off with a 25% duty cycle with a period of 4 seconds. This uses  $20\text{s} / 360\text{s/h} \times 25\% \times \approx 30\text{mA} \times 3.3\text{V} = 0.1375\text{mWh}$ , which is insignificant compared to the power used by the rest of the sensor module over the full period of operation.

### **3. DESIGN AND IMPLEMENTATION**

---

#### **3.2.8 Wristband and Electronics Enclosure**

Some of the sensor module's components require contact with the user's skin - namely the pulse and temperature sensors. The accelerometer must also be directly or indirectly affected by the user's motion. Chapter 2 discussed common locations on the body for the operation of each sensor, and from this the following justifications for a wrist based sensor module are made:

- Accelerometer - commonly located on the wrist for detecting sleep patterns in motions, with best results in this location (section 2.4).
- Temperature Sensor - measuring core body temperature is typically too invasive for this application, while skin temperature can be measured more easily. Research shows that distal skin temperature (such as measured on the wrist) has a strong relationship with the user's level of wakefulness (see section 2.5). Skin temperature is more greatly influenced by external conditions, and as such the data acquired requires more processing to be of a useful nature for sleep pattern detection.
- Pulse Sensor - the sensor used is a reflectance type pulse oximeter, and its use is not restricted to thin segments of flesh (e.g. the fingers or earlobes) as an absorption type sensor would. The sensor works best where blood flow is close to the surface of the skin, such as the forehead, lips, fingertips, tongue, and the wrist.

There are several consequences associated with a wrist based sensor module, such as requiring a secure method of attachment, and the possible exposure to undesirable moisture and temperature conditions; each of which will be discussed in this section.

The sensor module should be securely attached to the wrist to reduce motion artefacts - in this case, motion of the wrist relative to the sensor module. This is especially of concern for the pulse sensor where even slight changes in blood vessel situation in it's view cause significant disturbances in pulse detection; while the affect on acceleration would be negligible, and temperature would only be affected if air could flow between it and the user's skin. In contrast, the sensor module should also not be uncomfortably situated, which would not only be undesirable to the user (for both comfort and health

### 3.2 Sensor Module

reasons), but could also alter their conscious and unconscious behaviours, which may interfere with results.

Accessories that are worn on the wrist - such as watches and bracelets, typically wrap around the entire wrist, with some rigidity or elasticity to inhibit sliding around the wrist. The design of the sensor module's attachment method utilises both of these characteristics, with an elastic wristband and a rigid enclosure that spans almost the width of the wrist.

The required dimensions of the enclosure are determined from the size and layout of each component. Figure 3.15 shows the initial layout of the components within an arbitrary enclosure. Note that the pulse and temperature sensors are on the underside of the enclosure, and can not be seen in this figure.

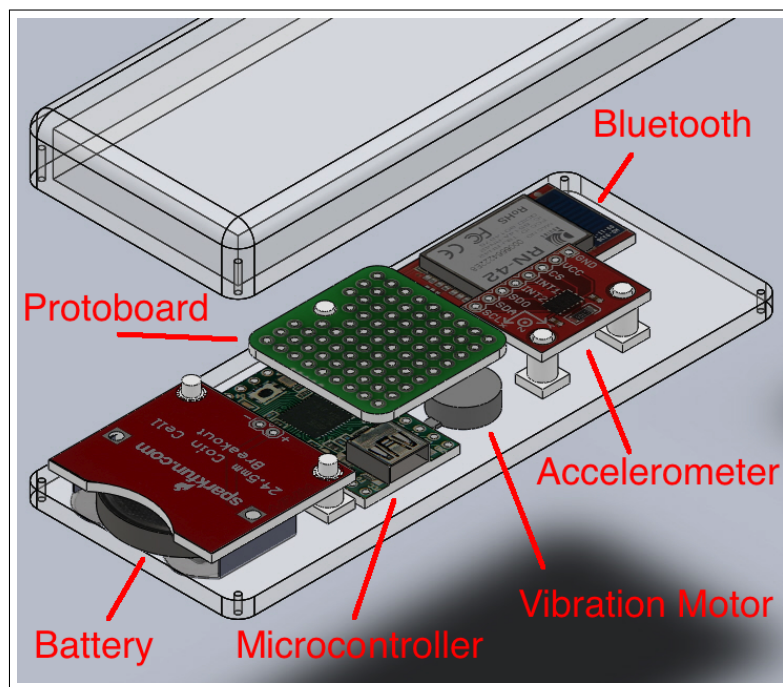


Figure 3.15: Component Layout - CAD

From this layout, the minimum enclosure size to fit all components was determined to be  $81\text{mm} \times 30\text{mm} \times 9\text{mm}$  (inner dimensions).

The enclosure with the closest dimensions to this minimum is shown in figure 3.16, with the dimensions  $90\text{mm} \times 50\text{mm} \times 16\text{mm}$  (outer dimensions). It is made of high impact ABS plastic with a lightly textured surface finish, which improves adherence

### **3. DESIGN AND IMPLEMENTATION**

---

with fixatives such as silicone paste. The four M3 screws that hold the case together can be seen in figure 3.16.



**Figure 3.16: Enclosure - Back Surface**

The final component layout shown in figure 3.17 is very similar to the initial CAD layout in figure 3.15. The purpose of the protoboard is now clearer, where nodes of wire are connected on the underside. Its components are:

- power and ground lines for each component, including decoupling capacitors
- I<sup>2</sup>C clock and data lines
- vibration motor control circuitry

The pulse and temperature sensors are the two components that require contact with the user's skin, and as such must be on the outside of the enclosure. This is achieved by mounting these sensors in a 5mm thick layer of silicone, as seen in figure 3.18. The pulse sensor has a thin, clear plastic cover to protect it from moisture while not inhibiting the transmission and reception of the light the sensor requires to function. The temperature sensor is covered by a very thin layer of silicone. The silicone has high thermal conductivity to augment the transfer of heat to and from the user. The silicone layer supporting these sensors is wide and flat with curved edges to maximise contact with the skin's surface, while not being uncomfortable. The wristband has a

### **3.2 Sensor Module**

---

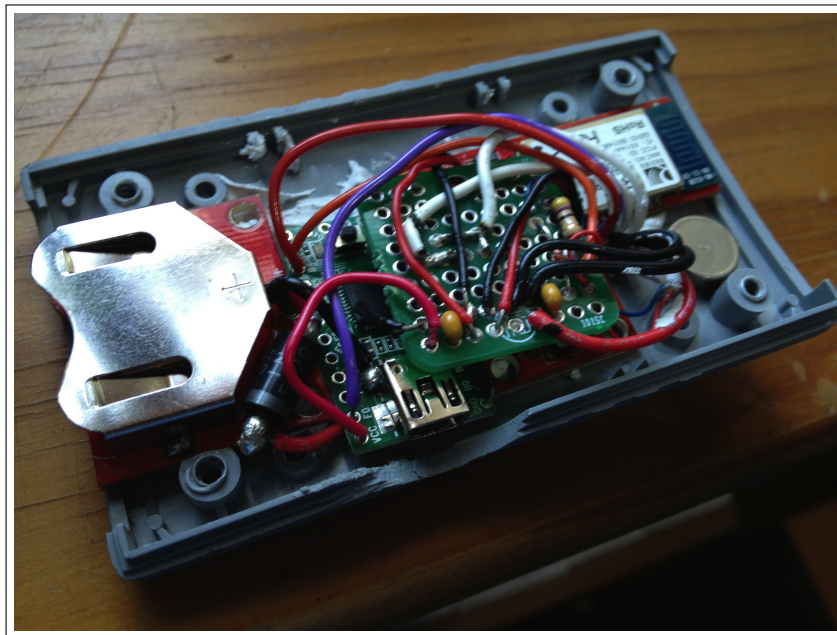


**Figure 3.17: Component Layout - Final**

hole cut to fit the silicone layer, and its material stretches to become under 5mm thick when worn, meaning the sensors protrude from the wristband material, as required for good skin contact. The snap fastener halves that are fixed to the enclosure attach to the wristband, serving to ensure the sensors protrude out and are not covered by the wristband.

Figure 3.20 shows the enclosure placed partially inside the wristband, through an incision between its two layers (right). The snap fasteners visible serve to keep the enclosure within the wristband (when clasped together). This design pulls the sensors (located on the inside of the wristband) into contact with the skin securely and not uncomfortably; while the rigid enclosure inhibits practically all sliding as the elastic wristband pulls it flat against the wrist.

Each of the components are operable in temperatures ranging from at most 0°C to at least 80°C, which easily includes the range for skin temperatures.

The battery can be easily inserted or removed from the back of the enclosure, which is sealable with a plastic cap. For microcontroller access during development, a hole was drilled into the side of the enclosure to fit a micro USB cable through, which can be sealed with a makeshift plastic cap.

### **3. DESIGN AND IMPLEMENTATION**

---



**Figure 3.18: Mounted Sensors** - Sensors attached to enclosure with adhesive silicone.



**Figure 3.19: Sensors Protruding from Wristband** - Attached with snap fasteners.



**Figure 3.20: Enclosure in Wristband - Snap Fasteners Unclasped**

### **3.3 Computer Module**

The purpose of this module is to receive and store the data sent from the sensor module. It must process and analyse this data, correlating characteristics to human sleep patterns and hence determine the user's current level of wakefulness. To achieve this, the module must have several hardware components:

- decent CPU and hard drive storage space - the computer must analyse the data close to real time, and storage of this data is advantageous for long term data analysis and comparison.
- bluetooth capability (internal or external) - for wireless communication with the sensor module.
- speakers and screen - the system uses these to effect the user's sleep, increasing wakefulness at the appropriate time.

The computer used to perform as part of the autonomous system for optimal human awakening is a MacBook Pro, which has bluetooth capabilities, a screen with adjustable

### **3. DESIGN AND IMPLEMENTATION**

---

brightness, speakers and both hardware and software suitable for performing processing and analysis of data.

This section describes the data collection and storage process, introduces the processing environment, and portrays the methods for waking the user with light and sound.

#### **3.3.1 Data Collection and Storage**

The collection and storage of data must be performed robustly to prevent corruption between the two wireless modules. Bluetooth is inherently robust with forward error correction (FEC) and retransmission of packets until acknowledged by the receiver (ARQ). Thus, the bluetooth transmission itself is unlikely to corrupt data, but measures must be put in place to prevent incomplete data transmission should either the sensor or computer module be disrupted (i.e. out of range, battery flat etc.).

The serial communication protocol used has two primary techniques to prevent data corruption. The first is that each packet begins with a start byte corresponding to the type of information the packet contained. This start byte also specified the length of the data packet - inherent to the type of information it contained (e.g. 6 bytes for an acceleration packet). If the start byte is unintentionally present in the data, an escape byte is placed before it so that the receiving end can interpret it as data, not a start byte.

The second technique is required because of the latency introduced to the wireless communication by the sniff mode enabled on the BlueSMiRF module. As mentioned in section 3.2.5, this mode checks if data needs to be sent or received at defined time intervals. If the check happens during the time when a packet is being sent from the microcontroller, it is likely that only some of that packet will be sent at this time - the rest is sent at the next "sniff". To prevent unwanted behaviour, the computer module detects the incomplete packet by comparing the number of bytes it contains with how many it should contain. If the packet is incomplete, it is stored and prepended to the next lot of data received, which contains the remaining bytes of the packet.

Once the data is obtained it is analysed and stored as binary float values, with no delimiter, in files named with the date of collection (of the form "YYYY-MM-DD.data"). The files are appended if they have already been created that day. These data files are accompanied by corresponding timestamp files with the same filename but

with the ".times" extension. For each data value stored, the timestamp of recording is also stored. The timestamp is determined by the time at connection (or reconnection) between the sensor and computer modules, plus a time offset corresponding to the data type.

By storing the data in this form it can be easily read into memory mapped arrays, where the computer can access data with minimal access time or memory resource requirements.

### **3.3.2 Processing**

One of the most efficient ways to utilise the OS X operating system for the real-time processing and analysis of the sensory data is with the Cocoa, Foundation, CoreData, QuartzCore, IOBluetooth frameworks. These frameworks are designed to work optimally with the computers hardware, and supply the developer with well documented, powerful API to perform the required processes.

Storing the recorded raw data allows for processing and analysis to be performed post-collection. This is especially important during development where these processes can change as improvements are made, meaning all recorded data can be re-analysed. Hence, recorded data never becomes redundant, and the need to record more data to test changes is negated.

Another advantage of archiving recordings is that MATLAB can be used for development of the processing and analysis procedures. MATLAB is a numerical computing environment and programming language that provides abundant high-level resources that simplify certain procedures. For example, MATLAB's comprehensive plotting functions are used to plot most of the data figures in the results chapter (chapter 5).

After testing processes in MATLAB, they are implemented in Objective-C for realtime use in the system. This data processing and analysis is discussed further in chapter 4.

### **3.3.3 Light and Sound**

The computer uses two processes to influence the user's sleeping patterns, the gradual introduction of light to the environment, and the emission of sound.

### **3. DESIGN AND IMPLEMENTATION**

---

The purpose of the gradually brightening light is to slowly increase the user's wakefulness. This is performed using the computer module's inbuilt screen, which should be positioned to direct most of the light towards the sleeping user.

When the analysis algorithm determines that the user requires waking, the screen brightens gradually. First, just before the screen is turned on with the lowest brightness level, it is filled with black colour. From here, the colour of the screen gradually changes its hue, saturation and value to become a light blue colour - still with the lowest screen brightness setting. Finally, the screen colour is maintained while the brightness of the screen increases gradually until full brightness is reached. The timing of this process is controlled so that maximum brightness should occur shortly before the user's optimal wake-time. As discussed in section 2.2.2, blue light is the most effective colour for increasing wakefulness.

As a backup, a typical alarm is sounded if it is detected that the user remains asleep, despite the presence of light and vibration.

#### **3.4 Summary**

This chapter introduced the design of the system, where each of the two modules requirements and capabilities were justified. The sensor module contains an accelerometer, temperature sensor and pulse oximeter for collecting data that can be correlated to particular stages of sleep. The processes performed by this module's microcontroller were also introduced, as well as the rechargeable coin cell power supply, bluetooth wireless communication process, and the enclosure designed to be worn on the wrist.

The computer module was also discussed, relating especially to the data storage procedure, the processing environment used, and the components used for influencing the user's sleep patterns.

## Chapter 4

# Processing and Correlation

### 4.1 Introduction

This chapter discusses the procedures used to interpret the raw data obtained from the sensors introduced in chapter 3. Each individual data source requires its own unique processing to form an estimate of the user's state of sleep. These estimates are then combined in a fusion process to produce a more accurate and robust result, from which the user's optimal wake-time may then be determined.

### 4.2 Acceleration

The features in the acceleration data that are indicative of the user's state of sleep are primarily:

- magnitude of motion
- counts of activity per epoch
- time since last motion

Before discussing how these features are detected and correlated to a sleep stage, it is important to realise that the raw data is not yet of an optimal form. The following processes are performed to reduce noise in the data, and convert it into a more meaningful form.

Firstly, the acceleration data is gathered from a 3-axis accelerometer, meaning each single acceleration is given as three orthogonal components. As discussed in section

## 4. PROCESSING AND CORRELATION

---

3.2.1, the direction of the acceleration is not useful as the system does not know (or need to know) the orientation of the sensor module. However, what is important, is the magnitude of acceleration - regardless of the direction of motion. Because the acceleration axes are orthogonal, the magnitude is obtained by taking the square root of the sum of each axis' acceleration squared, as in equation (4.1).

$$\bar{a}_g = \sqrt{a_x^2 + a_y^2 + a_z^2} \quad (4.1)$$

However, equation (4.1) leaves gravity unaccounted for. If the user is sleeping on a stationary platform, gravity will produce a constant acceleration which will be recorded by the accelerometer. Ideally, only the user's acceleration should be obtained, so the gravity vector must be removed from the raw data. If the direction of acceleration was needed, determining the gravity vector would require knowledge of the orientation of the sensor. However, because only the magnitude of acceleration is used, the magnitude of the gravity vector can be subtracted. Fortunately, the magnitude of the gravity vector is a well defined quantity:  $\approx 9.81m/s^2$ , or 1g. Subtracting this value from the total magnitude of acceleration provides a measure of the user's acceleration (equation (4.2)).

$$\bar{a}_u = |\bar{a}_g - 1| \quad (4.2)$$

For this equation to be accurate, the  $a_x, a_y, a_z$  accelerations are pre-scaled by the coefficients determined in the calibration procedure described in section 3.2.1. This scaling factor converts the accelerations to be measured in g's (where 1g is defined as the acceleration due to gravity), but the units of the accelerometer data aren't overly important, only the relative changes in magnitude.

The expected range of frequencies for the user's motion is around 0.5-5Hz (as discussed in section 2.4), so to mitigate any potential signal noise outside this frequency range, a bandpass filter is utilised.

Now that the accelerometer data is in a more usable form, important features and information must be extracted. Firstly, high accelerations are detected by simply comparing each magnitude with a threshold value. These accelerations are categorised as twitches, or more conscious motions, which are determined partially by the degree the acceleration exceeds the threshold.

### **4.3 Temperature**

---

For each sample that exceeds this threshold, its corresponding time is recorded. From this, a time interval pertaining to the length of time since the last significant motion can be determined, which is used in two ways. Firstly, it allows motions to be separated into discrete events, and secondly, long intervals are indicative of deep sleep and contribute to the weighting or ‘trust’ of the user’s sleep state.

The number of discrete motions in a time interval (termed ‘epoch’) is determined by the number of accelerations exceeding a threshold, that have also occurred at a minimum time interval since the last threshold exceeding acceleration.

The values of the previously mentioned classifying properties are as follows:

- acceleration threshold =  $0.05\text{g}$ . Determined experimentally, this value is sufficient to exceed three standard deviations of the noise level, and low enough to detect the majority of small twitches.
- epoch = 60 seconds. Suggested in literature (see section 2.4), this value represents the length of time for which motions are counted and grouped together, enabling a measure of motions per minute to be obtained dynamically.
- activity separation time = 1 second. Determined experimentally, this value is large enough to prevent single motions (i.e. the user moving their arm from a stationary position, to settle at another stationary position) to be counted multiple times, yet small enough to not miss quick, separate motions.

Validation of these values (and more) is performed through the use of time-lapse footage and manual sleep state estimates.

An estimate of the user’s sleep architecture is determined by combining these three features: magnitude of motion, counts of activity per epoch and time since last motion. Each is given a weighting for how well it correlates to a certain state of sleep over time.

## **4.3 Temperature**

The process of estimating the user’s sleep patterns from their changes in skin temperature is performed by analysing the magnitude of temperature, and its rate of change.

The key characteristic that is indicative of a wakeful state after a period of sleep is a significant drop in skin temperature, as discussed in section 2.5. However, because of

## **4. PROCESSING AND CORRELATION**

---

the expected artefacts introduced through changes in environmental temperature, the rate of change is required to differentiate causes of temperature variations.

Unlike the other sensors, the temperature sensor presents insignificant amounts of high frequency noise. In addition, the low frequency components of the signal are meaningful, meaning a filter is not required. The rate of change in temperature is determined from the raw temperature data through a form of differentiation. Each sample has a previous sample from 5 minutes prior subtracted from it, which is then passed through a low pass filter with a cutoff frequency at  $\frac{1}{900}$ Hz (30 minutes per oscillation). Both of these values were estimated from the literature studied showing that skin temperature changes quite slowly, and later confirmed as adequate through experimentation. The filter is necessary here because the rate of change in temperature is quite small, and the sensors resolution becomes a factor and discretisation is more considerable.

In estimating the state of sleep, a threshold was used to detect large negative change rates, and weighted with the relative temperature.

### **4.4 Heart Rate**

The raw data obtained from the pulse oximeter pertains to the oxygen content of the blood, which oscillates with each heart beat. Thus, some form of frequency analysis must be performed to detect the user's heart rate.

However, the raw signal will likely have some motion artefacts that correlate with the acceleration spikes detected by the accelerometer. These motions may result in slight changes of the sensor's positioning, and hence detect slightly different mean levels. This will appear as sudden drops or rises in the raw data, which should be filtered out.

The filtering of the raw data is performed using a Butterworth bandpass filter, with cutoff frequencies at 0.5Hz and 3Hz (30bpm and 180bpm - the expected range of heart rates). With this filtered data, a fast Fourier transform (FFT) was applied to detect the frequency components of the signal. Every 5 seconds, the data obtained in the last 10 seconds is analysed using the FFT, where the overlap should produce smoother results. Each time the data is transformed, the maximum frequency component is detected and recorded as the user's heart rate. The variation in this detected frequency from sample

to sample may be significant, introducing a high frequency noise component. As such, a low-pass filter is applied, with a cutoff at 1 minute per oscillation.

The features indicative of certain sleep states are (as discussed in section 2.6):

- higher heart rate - awake
- lower heart rate - deep sleep
- large variations in heart rate - light (REM)

With the information gathered, these features can be detected, and an estimate of the user's sleep state can be determined.

## 4.5 Estimate Fusion

With the estimates obtained through the analysis of the user's acceleration, skin temperature and heart rate, a more robust estimate of the user's sleeping patterns can be formed through their fusion.

Equation (4.3) is the underlying principle of this fusion, where  $E_k^a, E_k^t, E_k^h$  are the individual estimates from each data source;  $W_k^a, W_k^t, W_k^h$  are the weightings determined from the analysis of each data source, reflecting how much trust the algorithm places in its estimate; and  $w_a, w_t, w_h$  are the constant weightings for the estimates from each data source which are determined experimentally by observing how well the estimates match the expected sleep architecture (i.e. if a data source correlates poorly to the sleep stages, less weighting is given to its estimate). This equation is utilised at set intervals, where  $k$  represents the current estimation number. However, because the sample rates for each data source are different, the synchronisation of estimation times is difficult, and as such the most recent estimate from each data source is used.

$$E_k = \frac{w_a W_k^a E_k^a + w_t W_k^t E_k^t + w_h W_k^h E_k^h}{w_a W_k^a + w_t W_k^t + w_h W_k^h} \quad (4.3)$$

The next step in the fusion process is to filter this combined estimate. Each estimate has a relation to its previous, but this is not reflected in equation (4.3). One last bandpass filter is applied to better represent this time-dependance.

## **4. PROCESSING AND CORRELATION**

---

Finally, this continuous sleep state estimate is rounded to the nearest integer to form a discrete sleep architecture that is useful for controlling the system, and determining the optimal wake-time.

The optimal wake-time is during light sleep, typically after a period of brief motions or twitches (as discussed in section 2.4). The processes presented in this chapter supply the system with enough information to determine this time (if available) during the time frame the user specified as their desired waking schedule.

### **4.6 Summary**

This chapter has discussed the processing and analysis techniques utilised to form an estimate of the user's sleep state patterns. For each detection method, the features that must be observed in the data were described, as well as the processes developed to detect them. For example, the process of obtaining a measure of heart rate from the pulse oximetry data consisted of removing noise with a bandpass filter, and performing frequency domain analysis with a fast Fourier transform.

# **Chapter 5**

## **Results**

### **5.1 Introduction**

The implementation of the Automated System for Optimal Human Awakening has been discussed in detail in chapter 3, which presented the sensors used, the control techniques, the enclosure and physical components, wireless communication, and power supply. All of these details are important in implementing the system, but perhaps of greater importance to this thesis is how well the system design functions relative to its purpose.

This chapter presents the results of the correlation procedures, showing how well the data obtained from the system's sensors can be used to determine the user's state of sleep. The performance of the system is also discussed, in relation to comparisons with manually determined sleep state pattern estimates.

### **5.2 Correlation**

By nature, sleeping patterns vary from night to night, due to the large number of influencing factors. These can be environmental factors which are sensed by the human body, changes in physiological processes, the psychological state and much more. As such, no two nights will exhibit the same sleep properties, and hence multiple recordings using this system can not be portrayed easily in combination. For clarity, this section of the results presents the data obtained and analysed on a single night.

For reference, this night consists of the following important events:

## 5. RESULTS

---

- 12.10am - user dons the wristband containing the sensor module, and the system is turned on. Recording starts.
- 12.30am - user falls asleep.
- 3.25am - alarm wakes user.
- 3.45am - user falls asleep again.
- 5.48am - sunrise.
- 5.56am - light wakes user, who looks at clock and tries to go back to sleep.
- 6.30am - user gets up, turns off system and removes wristband. Recording stops.

These times were determined using the user's recollections (recorded immediately after rising at 6.30am), and time-lapse video footage of the user sleeping, see figure 5.1 for a graphical representation of the events stated above).

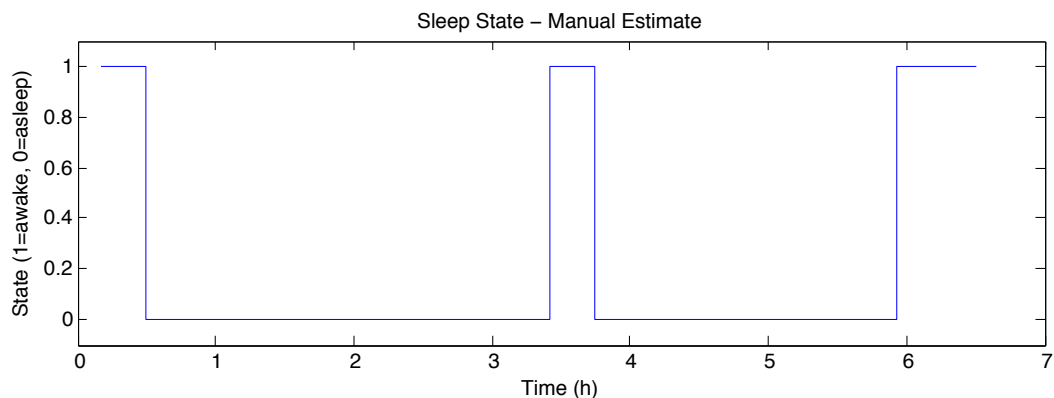


**Figure 5.1: Sleep State - Manual Estimation** - Wake times as determined through the user's recollections and time-lapse footage.

Note that an alarm was set to sound at 3.25am to compare the user's sleeping patterns when waking from a deep sleep to waking from a light sleep induced by ambient light (from the sun rising). 3.25am was determined to be one of the most likely times for deep sleep to occur based on prior recordings and analysis.

### 5.2.1 Actigraphy

The accelerometer data proved to be the most useful compared to that of the skin temperature and heart rate. The user's motions were accurately detected (based on time-lapse footage verification), and could be correlated to different states of sleep with greater trust.

Figure 5.2 portrays some of the process of correlating the user's acceleration to three different states of sleep: awake, light and deep. The magnitude of acceleration shown in figure 5.2a already indicates several features that can allow the viewer to deduce the user's state of sleep by visually assessing the graph. The frequent spikes suggest a lot of motion (i.e. user is awake); the isolated acceleration spikes suggest twitches or brief motions (i.e. user is experiencing a light sleep); and the long periods without significant motion suggest the user is in a deep sleep state. It is also apparent why filtering and a threshold value is required, due to the noise most clearly seen during periods without motion spikes. This noise is shown to be somewhat dependant on the gravity vector (i.e. the orientation of the sensor module), where its magnitude changes from time to time, usually after a motion from the user. An example of this is at around the 4.6 hour mark.

Figure 5.2b portrays more clearly the time intervals between significant accelerations. Because the analysis must be performed in real-time, it is necessary to determine this time interval when each acceleration sample is obtained. This data is used to obtain the activity counts shown in figure 5.2c, where the number of separate motions in each 60 second epoch are counted. The final sleep state estimate in figure 5.2d is determined from the combined information acquired from the previous three plots. This plot discretises the sleep cycle into 3 distinct stages, which is more useful in this system implementation than a continuous measurement.

### 5.2.2 Skin Temperature

The resulting sleep pattern estimates obtained from the analysis of skin temperature recordings tend to reflect the user's state of sleep to some degree. The expected drops in temperature during wakefulness (see research in section 2.5) were observed in the majority of recordings, as can be seen in figure 5.3. However, in some cases these

## 5. RESULTS

---

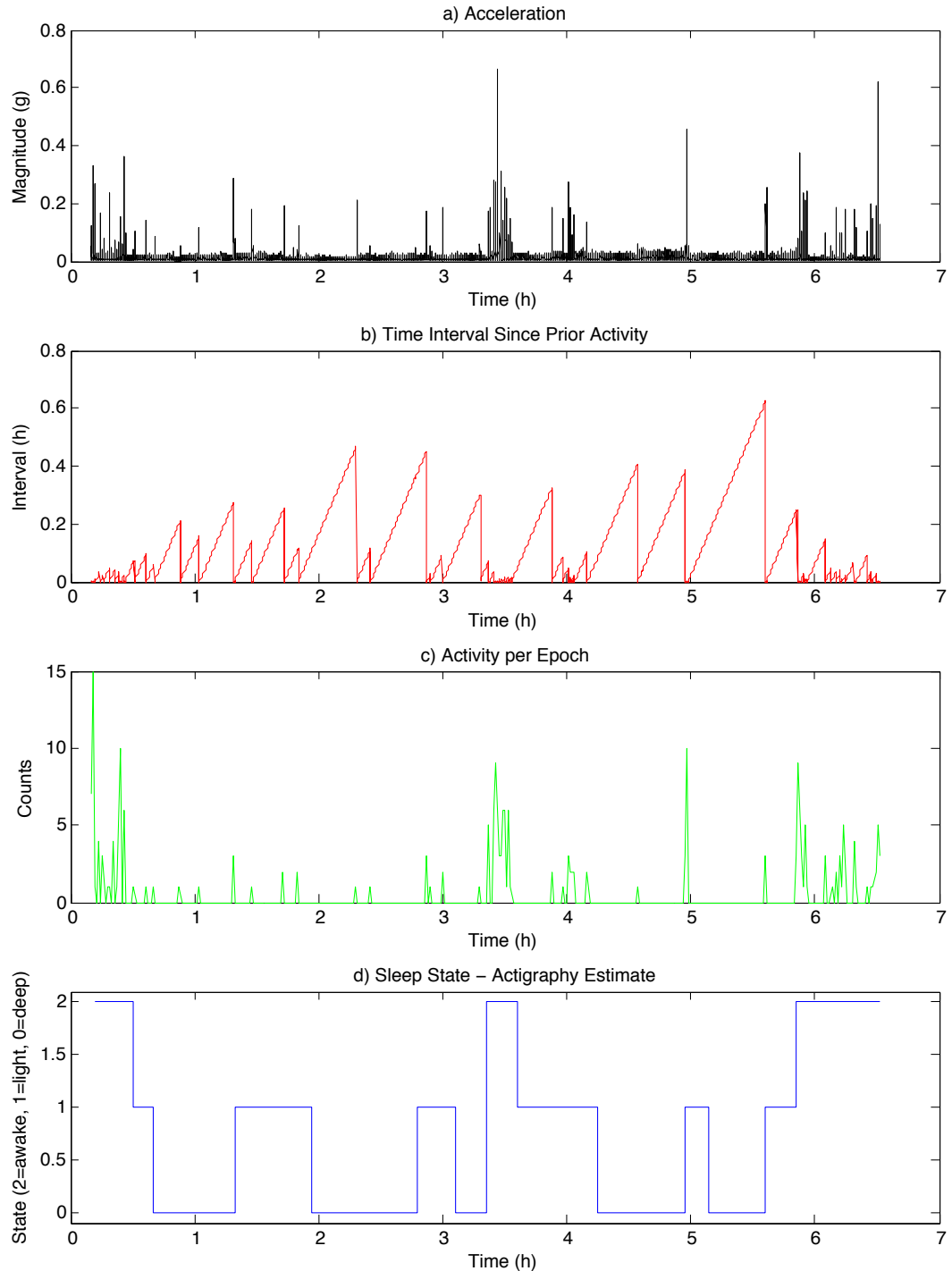


**Figure 5.2: Sleep State Estimation Process - Actigraphy** - First, the raw acceleration data is converted into the more useful form shown in plot a). Plot b) and c) portray two different properties obtained from the raw data, which are used to estimate the user's changes in sleep state as shown in plot d).

changes were difficult to distinguish from temperature changes resulting from environmental disturbances; such as the user moving their arm from beneath the bed covers. For example, figure 5.3 shows a sudden drop in skin temperature at around 5am - at the same time as an acceleration spike shown in figure 5.2. As there were few other motions for an extended period, this suggests that this first motion instigated the change in temperature.

Despite these factors, the sleep state estimate shown in figure 5.3c has some similarities to the known sleep architecture, where the awakening due to the alarm and that due to sunlight's influence are shown. However, there are several false positives; as is normally the case as observed in data sets from other nights. As such, this estimate is given a smaller weighting when fused with the estimates from the other data sources (section 5.2.4)

### 5.2.3 Heart Rate

The raw data obtained from the pulse oximeter contained the motion artefacts as expected, but also the much more frequent appearance of singular sample outliers. The cause of these outliers was partially identified as an insufficient decoupling of the bluetooth module with the microcontroller, which affected the ADC reference voltage during some (but not all) transmission periods. Both of these artefacts can be seen in figure 5.4.

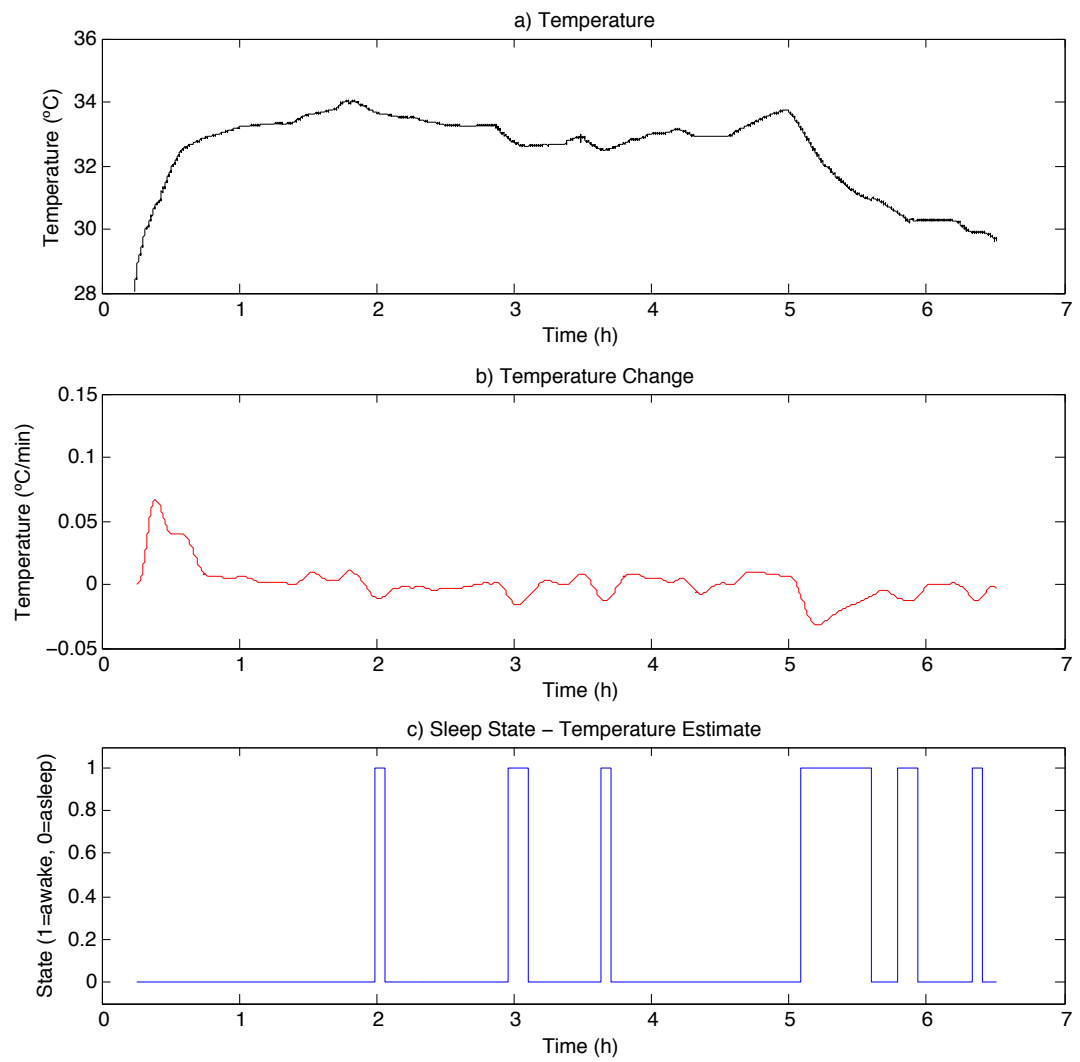
The heartbeat's influence is apparent on a smaller scale, as seen in figure 5.5 where both raw and filtered data is shown for comparison. The filter functions well, removing the low frequency components (slight rise and fall in average from 3.0795h to 3.084h), and some of the higher frequency components induced by the discretisation of the raw analogue signal.

Figure 5.6 portrays the heart rate detected throughout the night, as well as the user's estimated state of sleep. The rate of change in heart rate was not always a good indication of light sleep, potentially due to the significant variation inherent in the detection method and data quality. As such, the weighting given to this factor in determining the sleep state estimate was reduced.

Notice that in this case a rise in heart rate induced by the alarm at 3.25am is not apparent. This is sometimes the case where motion artefacts skew the interpretation

## 5. RESULTS

---



**Figure 5.3: Sleep State Estimation Process - Skin Temperature Correlation -**  
 Plot a) shows the raw data obtained from the temperature sensor, while figure b) shows the rate of change in temperature. The sleep state estimate obtained is shown in plot c).

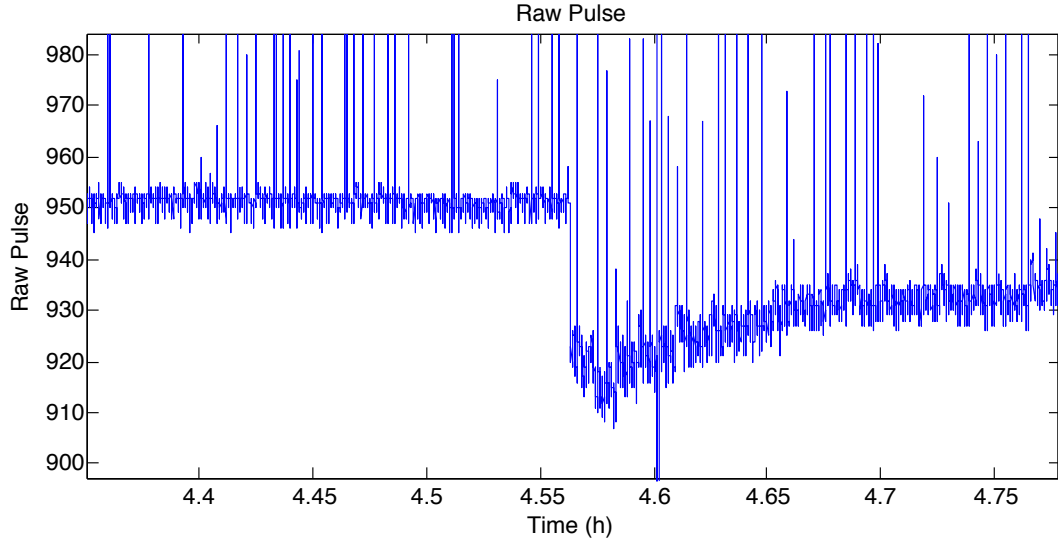


**Figure 5.4: Raw Oximeter Data Artefacts** - The motion artefact is the drop in mean signal level at 4.553h, corresponding to a spike of motion detected by the accelerometer. The other type of artefact is the large outlier spikes throughout the signal.

of the data. However, in most cases where the user was woken by an alarm, a rise in heartrate was detected.

This detection method often detects periods of wakefulness accurately, without few false positives.

### 5.2.4 Fused State Estimate

With an estimate of the user's sleep state obtained from each of the accelerometer, oximeter and temperature sensor acquired data, a fused estimate can be formed. Each of these estimates for this night can be seen in figure 5.7.

The estimate weightings  $w_a, w_t, w_h$  (introduced in section 4.5) were set at 0.8, 0.1 and 0.5 respectively, which were found experimentally to be the most appropriate values.

The fused estimate closely matches the expected sleep architecture based on the user's recollection (listed in section 5.2) and time-lapse footage that was recorded of the user sleeping (while wearing the sensor module). The time-lapse footage was useful for comparison with the motions detected through the accelerometer. Together, these two comparisons help validate the data and estimates obtained.

## 5. RESULTS

---

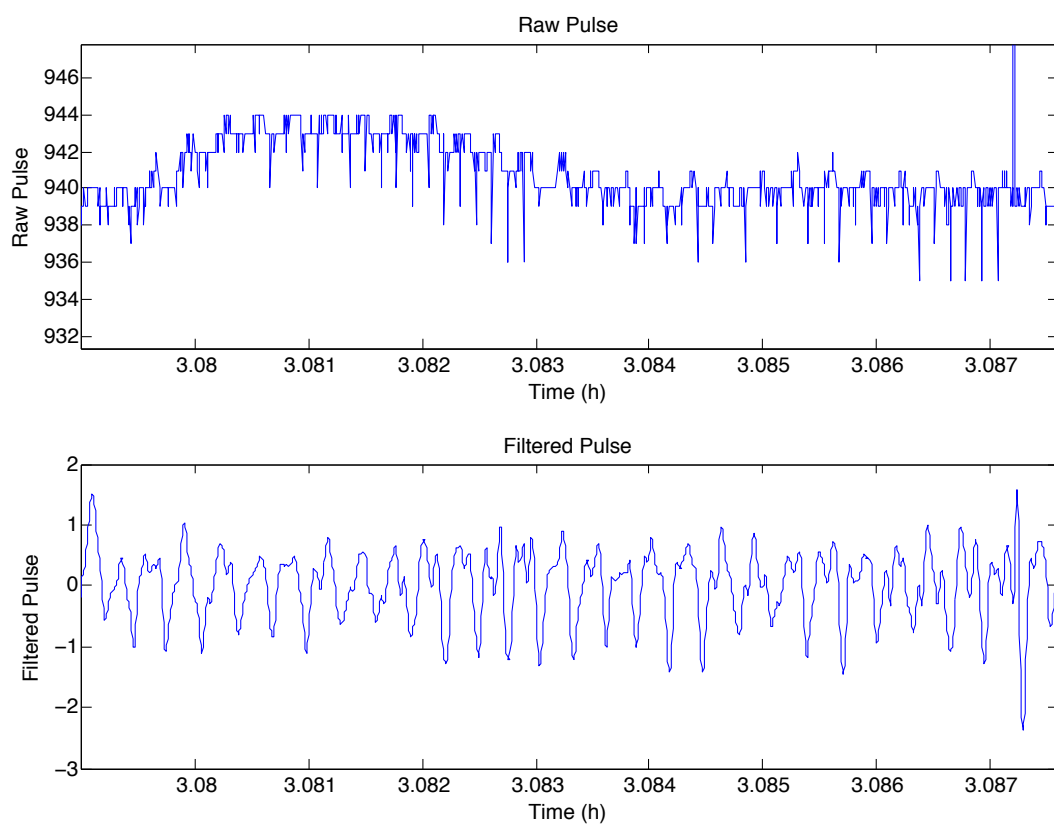


**Figure 5.5: Heart Pulses in Oximetry Data** - A 30 second period of a sleep recording, where the heart rate was detected to be around 60bpm throughout.

## 5.2 Correlation

---

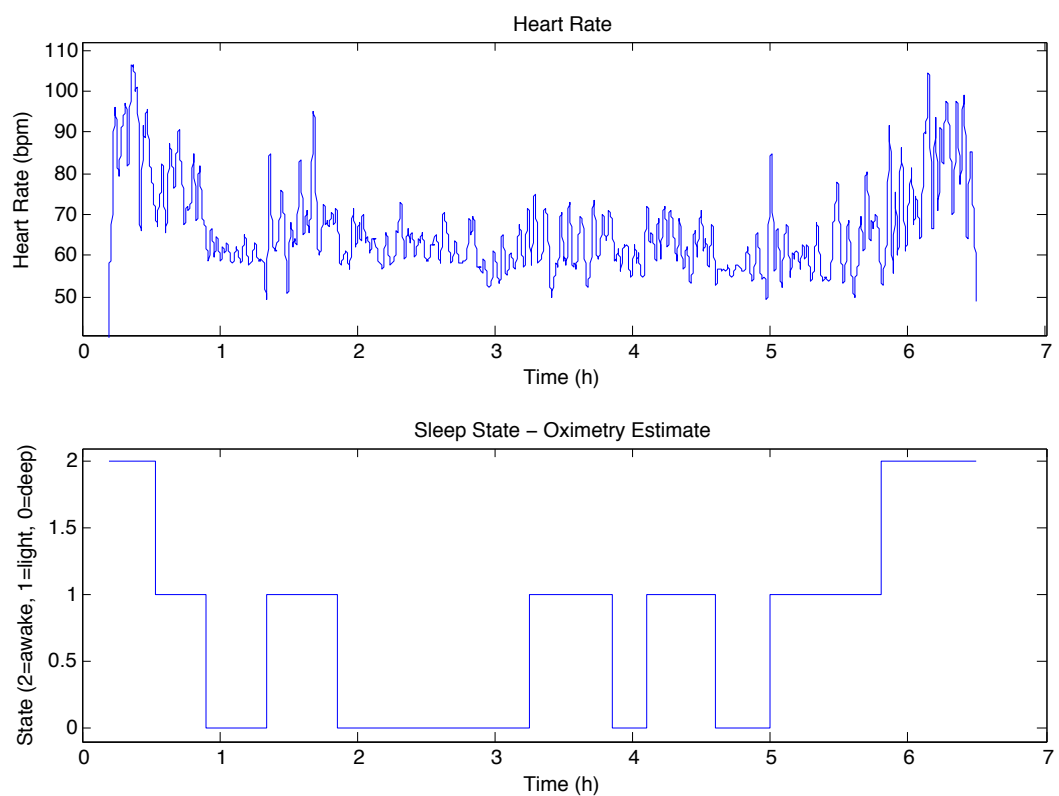


**Figure 5.6: Sleep State Estimation Process - Heart Rate Correlation** - The user's heart rate (top) is used to determine a sleep state estimate (bottom).

## 5. RESULTS

---

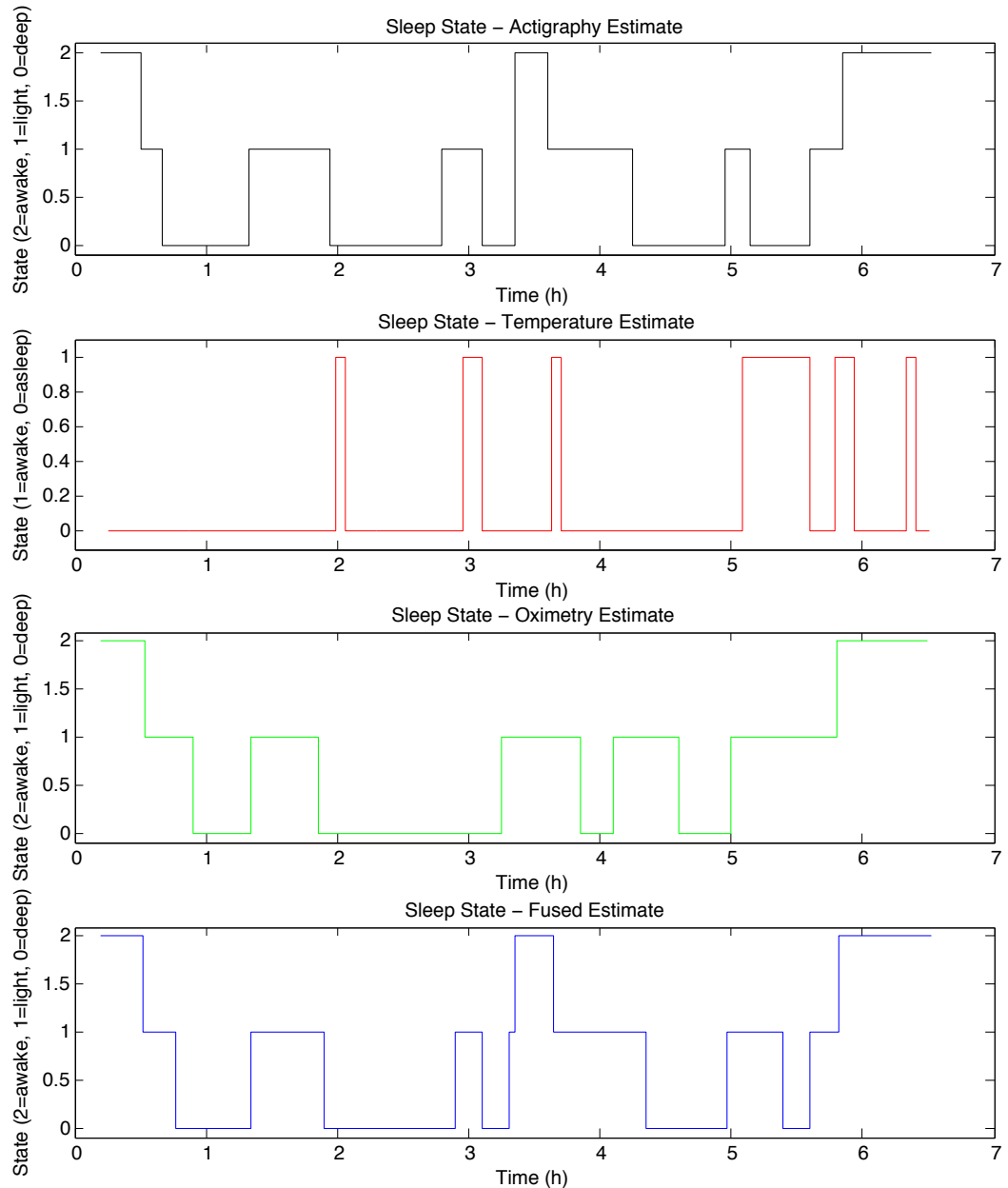


**Figure 5.7: Sleep State Estimate Fusion** - Acceleration, temperature and heartrate based estimates, and the resulting fused estimate.

## 5.3 Influencing Sleep

The effectiveness of the methods utilised to influence the user's sleep patterns is quite high. The first of these methods is the gradually increasing brightness of the computer screen light (whose purpose was to mimic the effects of a sunrise) produced similar changes in wakefulness. Figure 5.8 portrays a comparison between the accelerations detected for two different recordings, where the user woke after a sunrise (top plot), and after the computer light gradually lit (bottom plot). Very little motion is observed at the start of the plots, before light is introduced to the environment, after which some motion occurs with increasing frequency and magnitude.

This was repeated several times, with similar results, and further confirmation of this similarity from the user.

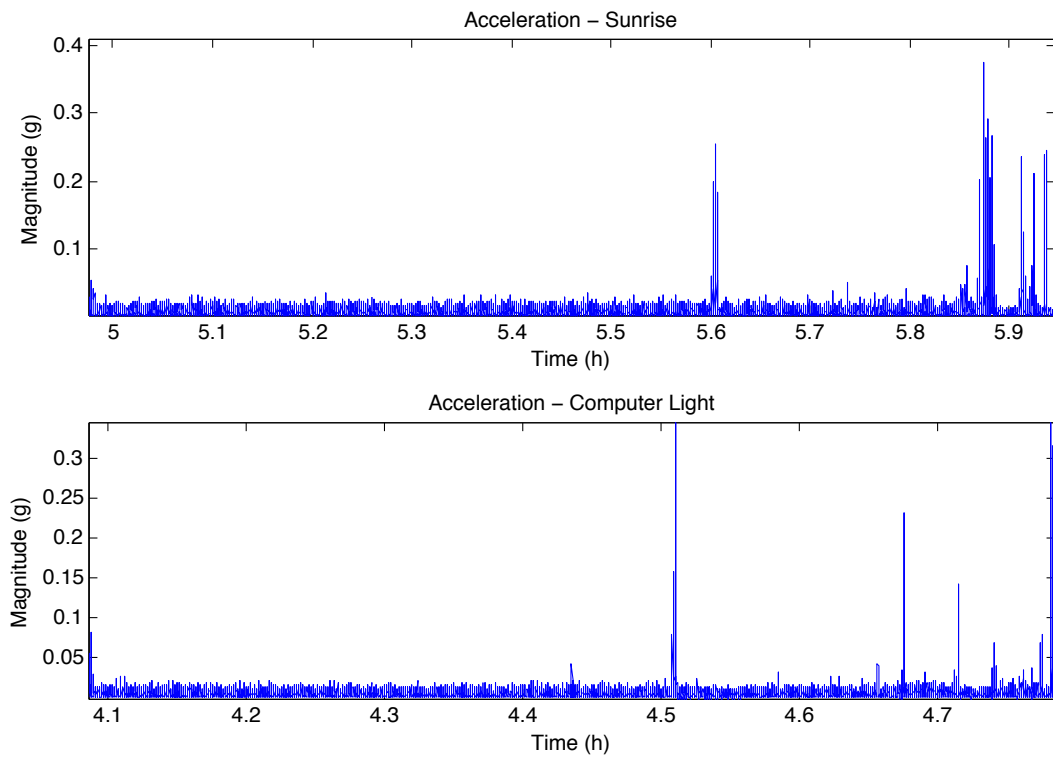


**Figure 5.8: Light's Influence** - A comparison of the motions induced by the gradual introduction of sunrise versus computer light.

The vibration motor in the sensor module woke the user in 76% (in 17 tests) of its

## **5. RESULTS**

---

uses as a less invasive alarm. In almost all cases where the vibration motor did not wake the user, the sleep state was estimated as deep sleep. From these tests, it was apparent that the use of the vibration motor was effective in all cases for which the computer light (or sunlight) was used to increase the user's wakefulness prior.

In the cases where the vibration motor did not fully wake the user, a backup alarm was emitted from the computer's speakers with a 100% success rate at waking the user.

### **5.4 Summary**

The results portrayed in this chapter demonstrate the effectiveness of the system implemented. For clarity, a single night's data and subsequent sleep state estimate was shown. The same process was performed 3 times, with 3 different users, where only once did the results show some significant differences to the manually determined sleep state estimate.

The methods employed to influence the user's sleep patterns were shown to be successful, where the user woke gradually with the gradual introduction of light and vibration (and sound if necessary).

# Chapter 6

## Discussion

This chapter briefly discusses the successfulness of the system design and the sleep state detection process, examining any issues with the results portrayed and discussed in chapter 5.

### 6.1 Sleep State Detection

The motion data collected from the accelerometer is very similar to that obtained with by other implementations discussed in section 2.4. The analysis procedures implemented performed as well as they were expected to, as portrayed and discussed in section 5.2.1.

The slight low frequency motions induced by breathing and translated to the wrist (dependent on arm position) had little effect on the analysis of the data, primarily because these motions typically consist of very small acceleration - especially so as breaths are normally shallower and slower during sleep. Similarly, if the wrist's motion is inhibited (e.g. the user rolling onto their arm), any twitches that occur are damped, but still present in the data and detectable.

The pulse oximeter could detect variations in reflected light due to changes in oxygen content of the blood with the heart beat, however the amplitude of this variation was often small in magnitude, and prone to noise. The attachment method of the sensor to the wrist was secure, so changes in ambient light produced no visible change in the detected signal, and movements were less likely to displace the sensor and obscure the

## **6. DISCUSSION**

---

heart rate data. While the wristband did not feel tight (material stretches to fit user), it may have obstructed some blood flow to the skin, affecting results.

The location of the sensor on the wrist made little difference, despite indications in the literature that high blood flow beneath the skin was of critical importance - it was anticipated locations over veins and arteries on the underside of the wrist would produce best results. However, blood flow IN the skin seemed to have more importance, where locations such as lips and ears produces high amplitude oscillations. Also supporting this hypothesis is the results from one particular test where the user had sunburnt skin on their wrist, producing at least 10 times the variation in reflected light amplitude associated with heart beats.

The temperature sensor detected the expected drop in skin temperature on the wrist when the user wakes, but had an undesirably slow heat transfer rate, where the cloth wristband seemed to act as a heat insulator. For the temperature analysis to work, the sudden environmental temperature changes should be recorded as higher frequency changes to those made by the body during the waking process, so that they can be distinguished and filtered from the signal.

An example of a sudden environmental temperature change is when the sensor module is moved under a blanket where the temperature is typically much warmer. Slow environmental temperature changes (e.g. typically gets colder approaching dawn) are of less concern, as they can be observed with a second temperature sensor in the computer module, and removed from the sensor module's temperature sensor data.

The methods used to validate and compare the sleep state estimates obtained were sufficient for the purpose of this thesis, but more detailed analysis of the systems performance would be beneficial. The time-lapse footage taken of the user sleeping required some ambient light in the room, and thus may have affected the user's sleeping patterns. There were also some psychological effects introduced by filming the user, where they often reported remembering the camera throughout the night, which caused a further increase in wakefulness.

### **6.2 System Design**

The goal of this thesis was not only to detect and influence the user's sleeping patterns to induce an optimal awakening, but also to implement a prototype for a commercially

## **6.2 System Design**

---

viable product. This section discusses the functionality of the system.

From the user's perspective, the system is very simple to use, requiring a wristband to be worn, and a computer to automatically analyse sleeping patterns. The sleep behaviour of the user is not physically affected by the system due to it's non-invasive nature, with a small, wireless profile.

Perhaps the only inconvenience was the need to change batteries relatively frequently. Despite the estimated 19hours of continuous operation (discussed in section 3.2.6), the batteries only lasted around 7 hours from full charge. The cause for this degradation is undetermined, but the operating time could be extended by running the sensor module in sleep mode where appropriate. Unfortunately after multiple uses, the batteries continued to reduce in power capacity, and had to be replaced for the system to be able to run the whole night.

In a commercial application, the device would only need to be functional before and during the period of time that the user is expected to wake, significantly reducing power requirements. For this thesis, extended recordings were made to demonstrate the sleep state estimation process.

Using bluetooth technology for the wireless communication proved to be very robust, only disconnecting when out of range or if the battery was exhausted. In combination with the specially designed data packet protocol used to communicate the sensory data to the computer module, no corrupted data was ever detected. On the sensor module, the bluetooth component's high power transmission procedure introduced some noise in the pulse oximetry data acquired (by affecting the ADC reference), because of insufficient power decoupling between the microcontroller and the bluetooth component. While not ideal, this noise could be filtered out of the oximetry data.

The components used to influence the user's sleeping patterns functioned as designed, and achieved their purpose. The vibration motor is small, but produces a noticeable vibration in the wristband when awake, which tends to wake the user gradually, and not harshly. The computer light was surprisingly bright, and it is easy to see how a specially designed light could be even more effective. Finally, the computer's speakers were easily capable of producing an alarm sound loud enough to wake the user from deep sleep if necessary.

## **6. DISCUSSION**

---

# **Chapter 7**

## **Conclusions**

This thesis set out to develop a proficient method for detecting and influencing human sleep patterns in order to induce an optimal awakening procedure. The unique approach of fusing three sleep state estimates obtained from the analysis of independent data sources has been shown to be effective.

This chapter summarises the contributions of this thesis, and highlights potential areas of future research.

### **7.1 Contributions**

The contributions of this thesis arise from the formulation of a unique approach for the detection of sleep state patterns using non-invasive methods; and the subsequent procedures designed to influence these sleeping patterns and induce an optimal awakening.

The major contributions made are:

- Individual sleep state estimates obtained from the analysis of accelerometer, pulse oximeter and temperature sensor data can then be fused to form a single, more robust sleep state estimate.
- An optimal wake-time can be determined from the sleep state estimate fusion process that has been developed.
- The sleep state estimate fusion process can be performed with a small, wireless device attached to the user's wrist that is portable and does not inhibit their natural behaviour.

## 7. CONCLUSIONS

---

- Wrist based pulse oximetry and skin temperature measurements can be analysed to determine changes in sleep state.
- The gradual introduction of blue light to a dark environment can be used to reliably increase a person's wakefulness.

### 7.2 Future Research

Recent years have seen several commercial and medical implementations of minimally invasive sleep state detection systems. This thesis has focused on developing a more robust detection method, and has identified potential areas requiring further development.

This thesis utilised three main sensors, but there are many others that could potentially be used to proficiently detect the user's state of sleep. For example, detecting electrodermal activity with passive current induction is a low power technique capable of detecting features indicative of certain sleep states, as discussed in section 2.8. This technique was initially considered for inclusion in this system, but was deemed beyond the scope of the thesis. Other detection methods that could be used include infra-red camera footage with computer vision analysis, microphone recording analysis, air flow (breath) sensor analysis, and more. There has been limited innovative research in this area, and improved analysis techniques may also be developed by, for example, researching further the time and frequency domain components of sensory data obtained.

Improved methods for influencing sleeping patterns may also be developed. An example of this is discussed in section 2.5 where the user's skin temperature is affected to increase the prevalence of deep sleep.

With respect to the system developed in this thesis, several improvements could be made to increase its successfulness. Firstly, it is worth noting that the sensor module implemented is a prototype, and that the miniaturisation and subsequent efficiency improvement achieved through designing a single PCB comprised of only the essential components is significant. This would not only reduce size and power requirements, but also increase durability and device lifetime.

The pulse oximeter could likely be improved by implementing an amplifier and bandpass filter in hardware, matched to characteristic amplitudes and frequencies of

blood oxygen content variation with the heart beat. This could allow the use of less intensive peak seeking algorithms, instead of requiring a fast Fourier transform.

The methods used in this thesis to compare the results with the user's actual sleep state are relatively basic, and it is recommended that the conclusions made in this thesis are further validated with comparisons from other sources such as medical actigraphic devices or polysomnograms.

### **7.3 Summary**

This thesis has produced a new method for detecting human sleep patterns, which can be utilised to determine an optimal wake-time. Several techniques useful for influencing these sleep patterns have been identified and implemented in a system designed for convenient and effective use. These developments portray desirable attributes for utilisation in both medical and commercial applications, warranting future research in this field.

## **7. CONCLUSIONS**

---

# References

- [1] AM Adami, M Pavel, TL Hayes, and CM Singer. Detection of movement in bed using unobtrusive load cell sensors. *Information Technology in Biomedicine, IEEE Transactions on*, 14(2):481490, Feb. 2010. doi: 10.1109/TITB.2008.2010701. 13
- [2] Sonia Ancoli-Israel, Roger Cole, Cathy Alessi, Mark Chambers, William Moorcroft, and Charles P Pollak. The role of actigraphy in the study of sleep and circadian rhythms. *Sleep*, 26(3):342392, May 2003. 10, 11
- [3] Yosef Ashkenazy, Plamen Ch. Ivanov, Shlomo Havlin, Chung-K Peng, Ary L. Goldberger, and H. Eugene Stanley. Magnitude and sign correlations in heartbeat fluctuations. *arXiv.org*, cond-mat.stat-mech:, May 2000. doi: 10.1103/PhysRevLett.86.1900. 16
- [4] J J M JJ Askenasy. Sleep disturbances in parkinsonism. *Journal of Neural Transmission*, 110(2):125150, Jan. 2003. doi: 10.1007/s007020300001. 9
- [5] F i Baque. *i Baque: E., and deBons, M.(1983). Electrodermal asymmetry... - Google Scholar.* 18, 20
- [6] A A Borbely. Effects of light on sleep and activity rhythms. *Progress in neurobiology*, 10(1):131, 1978. 2
- [7] R Broughton, J Fleming, and J Fleetham. Home assessment of sleep disorders by portable monitoring. *Journal of Clinical Neurophysiology*, 13(4):272284, Jun. 1996. 10
- [8] G M Budd. Skin temperature, thermal comfort, sweating, clothing and activity of men slogging in antarctica. *The Journal of physiology*, 186(1):201215, Sep. 1966. 14
- [9] Chiara Cirelli and Giulio Tononi. Is sleep essential? *PLoS Biology*, 6(8):e216e216, Aug. 2008. doi: 10.1371/journal.pbio.0060216. 2, 7
- [10] C Eisdorfer, H O Doerr, and W Follette. Electrodermal reactivity: an analysis by age and sex. *Journal of human stress*, 6(4):3942, Dec. 1980. doi: 10.1080/0097840X.1980.9936107. 19
- [11] Mona El-Sheikh. *Sleep and Development. Familial and Socio-Cultural Considerations.* Feb. 2011. 9
- [12] D C DC Fowles, M J MJ Christie, R R Edelberg, W W WW Grings, D T DT Lykken, and P H PH Venables. Committee report. publication recommendations for electrodermal measurements. *Psychophysiology*, 18(3):232239, Apr. 1981. doi: 10.1111/j.1469-8986.1981.tb03024.x. 19
- [13] R Fronczek, R J E M Raymann, S Overeem, N Romeijn, J G van Dijk, G J Lammers, and E J W Van Someren. Manipulation of skin temperature improves nocturnal sleep in narcolepsy.

## REFERENCES

---

- Journal of Neurology, Neurosurgery and Psychiatry*, 79(12):13541357, Dec. 2008. doi: 10.1136/jnnp.2008.143610. 14
- [14] A Jarrett. *Jarrett: Physiology and Pathophysiology of the Skin:... - Google Scholar*. 1978. 19
- [15] Biren B BB Kamdar, Dale M DM Needham, and Nancy A NA Collop. Sleep deprivation in critical illness: its role in physical and psychological recovery. *Journal of Intensive Care Medicine*, 27(2):97111, Feb. 2012. doi: 10.1177/0885066610394322. 8
- [16] Jan W Kantelhardt, Yosef Ashkenazy, Plamen Ch. Ivanov, Armin Bunde, Shlomo Havlin, Thomas Penzel, Jorg-Hermann Peter, and H. Eugene Stanley. Characterization of sleep stages by correlations of heartbeat increments. *arXiv.org*, cond-mat.stat-mech, Dec. 2000. doi: 10.1103/PhysRevE.65.051908. 16, 17
- [17] A J Koumans, B Tursky, and P Solomon. Electrodermal levels and fluctuations during normal sleep. *Psychophysiology*, 5(3):300306, Nov. 1968. doi: 10.1111/j.1469-8986.1968.tb02826.x. 18
- [18] Jaakko Malmivuo and Robert Plonsey. *Bioelectromagnetism. Principles and Applications of Bioelectric and Biomagnetic Fields*. Oxford University Press, USA, Jul. 1995. URL <http://www.bem.fi/book/index.htm>. 18
- [19] Andrew P McDowell, Mark Donnelly, Chris D Nugent, and Michael McGrath. Passive sleep actigraphy: Evaluating a non-contact method of monitoring sleep. *ICOST*, page 157164, 2012. doi: 10.1007/978-3-642-30779-9\_20. 12, 13
- [20] H Møgaard, K E Srensen, and P Bjerregaard. Circadian variation and influence of risk factors on heart rate variability in healthy subjects. *The American Journal of Cardiology*, 68(8):777784, Sep. 1991. 14
- [21] Lucy A LA Newman, Marquis T MT Walker, R Lane RL Brown, Thomas W TW Cronin, and Phyllis R PR Robinson. Melanopsin forms a functional short-wavelength photopigment. *Biochemistry (Washington)*, 42(44):1273412738, Nov. 2003. doi: 10.1021/bi035418z. 9
- [22] Jean Paquet, Anna Kawinska, and Julie Carrier. Wake detection capacity of actigraphy during sleep. *Sleep*, 30(10):13621369, Oct. 2007. 11
- [23] C.-K. Peng, J Mietus, J Hausdorff, S Havlin, H Stanley, and A Goldberger. Long-range anticorrelations and non-gaussian behavior of the heartbeat. *Physical Review Letters*, 70(9):13431346, Mar. 1993. doi: 10.1103/PhysRevLett.70.1343. 16
- [24] Pedro Pires, Teresa Paiva, and Joo Sanches. Sleep/wakefulness state from actigraphy. *IbPRIA*, page 362369, 2009. doi: 10.1007/978-3-642-02172-5\_47. 10, 11
- [25] Ming-Zher Poh, Nicholas C Swenson, and Rosalind W Picard. A wearable sensor for unobtrusive, long-term assessment of electrodermal activity. *IEEE transactions on bio-medical engineering*,

---

## REFERENCES

- 57(5):12431252, May 2010. doi: 10.1109/TBME.2009.2038487. 20, 21
- [26] Yuan Qi Yuan Qi and RW Picard. Context-sensitive bayesian classifiers and application to mouse pressure pattern classification. *International Conference on Pattern Recognition. Proceedings*, 3:448443, Aug. 2002. doi: 10.1109/ICPR.2002.1047973. 19
- [27] Jean-Claude Roy, Wolfram Boucsein, Don C Fowles, and John Editors Gruzelier, editors. *Progress in Electrodermal Research (Nato Science Series A: (closed))*. Springer, 1 edition, Oct. 1993. 19
- [28] S Schmidt and H Walach. *Electrodermal Activity (EDA): State-of-the-Art Measurement and Techniques for Parapsychological Purposes*. JOURNAL, 1999. URL [http://www.thefreelibrary.com/ELECTRODERMAL+ACTIVITY+\(EDA\)+---+STATE-OF-THE-ART+MEASUREMENT+AND...-a067718670](http://www.thefreelibrary.com/ELECTRODERMAL+ACTIVITY+(EDA)+---+STATE-OF-THE-ART+MEASUREMENT+AND...-a067718670). 19, 20, 21
- [29] Vijay Kumar Sharma. Adaptive significance of circadian clocks. *Chronobiology international*, 20(6):901919, Nov. 2003. doi: 10.1081/CBI-120026099. 7, 8
- [30] Michael H Silber, Sonia Ancoli-Israel, Michael H Bonnet, Sudhansu Chokroverty, Madeleine M Grigg-Damberger, Max Hirshkowitz, Sheldon Kapen, Sharon A Keenan, Meir H Kryger, Thomas Penzel, and et al. The visual scoring of sleep in adults. *Journal of clinical sleep medicine : JCSM : official publication of the American Academy of Sleep Medicine*, 3(2):121131, Mar. 2007. 8
- [31] Sebastijan Sprager, Denis Donlagic, and Damjan Zazula. *Heartbeat detection applying activity index on optical interferometric signal*. World Scientific and Engineering Academy and Society (WSEAS, Apr. 2012. 18
- [32] Travis H TH Turner, Sean P A SP Drummond, Jennifer S JS Salamat, and Gregory G GG Brown. Effects of 42 hr of total sleep deprivation on component processes of verbal working memory. *Neuropsychology*, 21(6):787795, Oct. 2007. doi: 10.1037/0894-4105.21.6.787. 7
- [33] KOZLOV VALERIY. Method and system for sleep monitoring, regulation and planning. (US201007484032011230790): A61B 5/ 11 A I; A61B 5/ 00 A I, Sep. 2011. 12
- [34] E J Van Someren, R H Lazeron, B F Vonk, M Mirmiran, and D F Swaab. Gravitational artefact in frequency spectra of movement acceleration: implications for actigraphy in young and elderly subjects. *Journal of neuroscience methods*, 65(1):5562, Mar. 1996. 11
- [35] EJW Van Someren. Sciencedirect.com - progress in brain research - mechanisms and functions of coupling between sleep and temperature rhythms. *Progress in brain research*, 2006. 13, 14, 15, 31
- [36] W F Waters, R L Koresko, G V Rossie, and S A Hackley. Short-, medium-, and long-term relationships among meteorological and electrodermal variables. *Psychophysiology*, 16(5):445451, Sep. 1979.

## REFERENCES

---

- doi: 10.1111/j.1469-8986.1979.tb01502. [37] Rolf Weitkunat. *Digital biosignal processing*. Elsevier Science Ltd, 1991. 20 x. 18

## **Declaration**

I herewith declare that I have produced this thesis without the prohibited assistance of third parties and without making use of aids other than those specified; notions taken over directly or indirectly from other sources have been identified as such. This thesis has not previously been presented in identical or similar form to the University of Sydney, or other institutes of higher learning.

The thesis work was conducted from March to November of 2012 under the supervision of Stefan Williams at the University of Sydney.

Daniel Vogelnest